6-2020

Multiscale Model for Hurricane Evacuation and Fuel Shortage

Sirish Namilae
Embry-Riddle Aeronautical University

Dahai Liu
Embry-Riddle Aeronautical University

Scott Parr
Embry-Riddle Aeronautical University

MULTISCALE MODEL FOR HURRICANE EVACUATION AND FUEL SHORTAGE

FINAL REPORT

JUNE 2020

SIRISH NAMILAE, DAHAI LIU & SCOTT PARR

US DEPARTMENT OF TRANSPORTATION GRANT 69A3551747125

DISCLAIMER

The contents of this report reflect the views of the authors, who are responsible for the facts and the accuracy of the information presented herein. This document is disseminated under the sponsorship of the Department of Transportation, University Transportation Centers Program, in the interest of information exchange. The U.S. Government assumes no liability for the contents or use thereof.

1. Report No.	2. Government Accession No.	3. Recipient's Catalog No.
4. Title and Subtitle Multiscale Model for Hurricane Evacuation and Fuel Shortage		5. Report Date JUNE 2020 6. Source Organization Code
7. Author(s) SIRISH NAMILAE, DAHAI LIU AND SCOTT PARR		8. Source Organization Report No. CATM-2020-R2-ERAU
9. Performing Organization Name and Address Center for Advanced Transportation Mobility Transportation Institute 1601 E. Market Street Greensboro, NC 27411		10. Work Unit No. (TRAIS) 11. Contract or Grant No. 69A3551747125
12. Sponsoring Agency Name and Address University Transportation Centers Program (RDT-30) Office of the Secretary of Transportation–Research U.S. Department of Transportation 1200 New Jersey Avenue, SE Washington, DC 20590-0001		13. Type of Report and Period Covered Final Report: FEB 2019-JUNE 2020 14. Sponsoring Agency Code USDOT/OST-R/CATM
15. Supplementary Notes:		

16. Abstract

Hurricanes are powerful agents of destruction with significant socioeconomic impacts. High-volume mass evacuations, disruptions to the supply chain, and fuel hoarding from non-evacuees have led to localized fuel shortages lasting several days during recent hurricanes. Hurricane Irma in 2017, resulted in the largest evacuation in the nation affecting nearly 6.5 million people and saw widespread fuel shortages throughout the state of Florida. While news reports mention fuel shortages in several past hurricanes, the crowd source platform Gasbuddy has quantified the fuel shortages in the recent hurricanes. The analysis of this fuel shortage data suggested fuel shortages exhibited characteristics of an epidemic. Fundamentally, as fueling stations were depleted, the latent demand spread to neighboring stations and propagated throughout the community, similar to an epidemiological outbreak. In this paper, a Susceptible- Infected –Recovered (SIR) epidemic model was developed to study the evolution of fuel shortage during a hurricane evacuation. Within this framework, an optimal control theory was applied to identify an effective intervention strategy. Further, the study found a linear correlation between traffic demand during the evacuation of Hurricane Irma and the resulting fuel shortage data from Gasbuddy. This correlation was used in conjunction with the State-wide Regional Evacuation Study Program (SRESP) surveys to estimate the evacuation traffic and fuel shortages for potential hurricanes affecting south Florida. The epidemiological SIR dynamics and optimal control methodology was applied to analyze the fuel shortage predictions and to develop an effective refueling strategy.

17. Key Words

Hurricane evacuation, Fuel shortage, Epidemic model, Optimal control

18. Distribution Statement

Unrestricted; Document is available to the public through the National Technical Information Service; Springfield, VT.

19. Security Classif. (of this report)	20. Security Classif. (of this page)	21. No. of Pages	22. Price
Unclassified	Unclassified	**79**	…

TABLE OF CONTENTS

EXECUTIVE SUMMARY

Hurricanes are powerful agents of destruction with significant socioeconomic impacts. A persistent problem due to the large-scale evacuations during hurricanes in the southeastern United States is the fuel shortages during the evacuation. High-volume mass evacuations, disruptions to the supply chain, and fuel hoarding from non-evacuees have led to localized fuel shortages lasting several days during recent hurricanes. Hurricane Irma in 2017, resulted in the largest evacuation in the nation affecting nearly 6.5 million people and saw widespread fuel shortages throughout the state of Florida. While news reports mention fuel shortages in several past hurricanes, the crowd source platform Gasbuddy has quantified the fuel shortages in the recent hurricanes. The analysis of this fuel shortage data suggested fuel shortages exhibited characteristics of an epidemic. Fundamentally, as fuelling stations were depleted, the latent demand spread to neighboring stations and propagated throughout the community, similar to an epidemiological outbreak. In this paper, a Susceptible- Infected – Recovered (SIR) epidemic model was developed to study the evolution of fuel shortage during a hurricane evacuation.

Computational models can aid in emergency preparedness and help mitigate the impacts of hurricanes. We have modeled the hurricane fuel shortages using the SIR epidemic model. We utilize the crowd-sourced data corresponding to Hurricane Irma and Florence to parametrize the model. An estimation technique based on Unscented Kalman filter (UKF) is employed to evaluate the SIR dynamic parameters. An optimal control approach for refueling based on a vaccination analogue is presented to effectively reduce the fuel shortages under a resource constraint. We find the basic reproduction number corresponding to fuel shortages in Miami

during Hurricane Irma to be 3.98. Our control model estimates the duration and the level of intervention required to mitigate the fuel shortage epidemic.

Further, the study found a linear correlation between traffic demand during the evacuation of Hurricane Irma and the resulting fuel shortage data from Gasbuddy. This correlation was used in conjunction with the State-wide Regional Evacuation Study Program (SRESP) surveys to estimate the evacuation traffic and fuel shortages for potential hurricanes affecting south Florida. The epidemiological SIR dynamics and optimal control methodology was applied to analyze the fuel shortage predictions and to develop an effective refueling strategy. Results indicate that evacuation of Miami Dade County in the event of a Category 3 hurricane landfall in the region, could lead to fuel shortages in up to 90 percent of the refueling stations in the region. The model indicates that this can be reduced to 28 percent by providing relief to 75 percent of the gas stations during the first two days of the evacuation.

CHAPTER 1. FUEL SHORTAGES DURING HURRICANES: EPIDEMIOLOGICAL MODELING AND OPTIMAL CONTROL

(*This chapter has appeared as a research paper in plos one*)

INTRODUCTION

Hurricanes are a periodic socio-economic threat for population centers in coastal areas globally. There is evidence for increased hurricane activity in the industrial era [1], and a rise in the number of high-intensity hurricanes over the past four decades [2]. Hurricanes have a severe socio-economic effect over extended geographic areas and impact the health and safety of residents in coastal regions like Florida. Computational modeling integrated with new social media data sources can assist in emergency preparation and evacuation efforts which save lives.

In the past decade, hurricanes impacting the Southeastern United States have led to high volume evacuations. The 2017 evacuation from Hurricane Irma has been referred to as the largest evacuation in the history of the nation. During this hurricane, twenty-three counties in Florida issued mandatory evacuation orders, and the remaining forty-four counties placed voluntary orders. Analysis of Hurricane Irma traffic data obtained from the Florida Department of Transportation (FDOT) indicates a net exodus of 550,000 vehicles from the southern parts of Florida. It is estimated that approximately 6.8 million Floridians and tourists took to the roads in the days leading up to the storm [3]. Such mass evacuations have also been observed during Hurricane Florence [4], affecting North and South Carolinas, as well as during Hurricane Michael [5]. Hurricane evacuees tend to make longer, intercity

trips to stay with friends and family outside the impacted area and to completely move out of the storm path [6].

The high-volume mass evacuations, disruptions to the supply chain, long distances traveled, and fuel hoarding from non-evacuees have led to localized fuel shortages lasting several days and a cascade of problems in hurricane-affected areas. For example, evacuation during Hurricane Irma created a widespread fuel shortage problems days before the hurricane's landfall for most of Florida and especially for South Florida. The fuel shortage problems gave rise to various other issues such as an unpredictable increase in fuel prices that exasperate and hinder evacuees living in low-income areas, traffic congestion on the highways due to stranded vehicles, and difficulties with emergency and medical transportation needs [3]. Understanding the characteristics of fuel shortage during hurricane evacuation is crucial to the mitigation of this problem and reducing the casualties caused by an imminent hurricane. The data explosion from social media enables new analysis approaches for this problem. For example, a recent study examines twitter data to predict fuel shortages during disasters [7].

While news reports have documented fuel shortages during the past hurricanes, crowd-sourced data from the social media platform Gasbuddy [8] has quantified the shortages during recent hurricanes. The progression of fuel shortage through a geographic area and the return to normal fuel supply has similarities with the spread of infectious diseases. For example, a refueling station in the vicinity of another station that is out of gas is more likely to be depleted of fuel soon, similar to infectious disease spread. Sociologists and computational scientists have long studied social events using biological models of

infectious disease spread. Modeling interconnected social events as contagion leads to the analysis of these events in a new light. For example, a recent study by Towers et al [9] utilized epidemic modeling to examine mass killings related to gun violence and found that the likelihood of a mass killing increased because of a preceding occurrence of a similar event. Contagious disease modeling has been used to study several social phenomena that show epidemic like behavior such as: election campaign donations [10], spread of emotional influence in social media [11], suicidal ideation [12], spread of web malware [13], social contagion of altruism [14], etc. Recent studies have combined the biological and social contagious behaviors, e.g. Fu and coworkers [15] studied the interaction between the spread of the influenza infection, and the corresponding social media trends about flu-vaccine. These studies point to the success of epidemiological models in examining the dynamics of problems involving social contagion.

The well-studied classical compartmental epidemic models used in most of the above studies such as SIS (Susceptible-Infected-Susceptible), SIR (Susceptible-Infected-Recovered) and SIRS (Susceptible-Infected-Recovered-Susceptible) divide the host population into susceptible, infected and recovered compartments with a set of differential equations describing dynamics between these different compartments [16]. In this study, we apply the SIR dynamics to model fuel shortage during hurricane evacuation as an epidemic and examine the infection dynamics as shown in the schematic in FIG 1. We further apply optimal control theory to determine an optimal refueling strategy utilizing an SIR with vaccination analogue to estimate the refueling needs to mitigate the epidemic, subject to resource constraints.

We utilize the data from the crowd sourced platform Gasbuddy for Hurricane Irma to parametrize the model. The unique advantage of this data source is the easy access to the on-the-fly data as the evacuation and fuel shortages are evolving during a hurricane. While the Gasbuddy fuel shortage data exhibit the characteristics of an epidemic, the optimal refueling model is based on a time invariant continuous SIR model represented by continuous ordinary differential equations [17, 18]. To address this problem, we use the Unscented Kalman Filter (UKF) algorithm to numerically estimate the SIR model parameters that characterize the dynamics as a continuous SIR model, while closely resembling the fuel shortage empirical data. To the best of our knowledge, this is the first application of epidemiological modeling and optimal control algorithms to the problem of fuel shortages during hurricanes. The mathematical development for the problem is presented first, followed by the results and discussions.

METHODS

Data Sources

The fuel shortage data for this study were obtained from Gasbuddy news releases during evacuation due to Hurricanes Irma and Florence. Gasbuddy is an online database containing vital roadside information on more than 150,000 fuel stations [8]. Gasbuddy played a crucial role during Hurricanes Irma and Florence by connecting evacuees and providing real-time information on fuel availability in the affected areas during the evacuation. A recent article in The Wall Street Journal reported that the Gasbuddy Mobile app was downloaded 300,000 times during the events leading up to Hurricane Irma, compared to 30,000 times on a typical day [19]. One problem with crowd sourced data is the

reliability of the data. Gasbuddy cross-checks the reported data with the user's location information to improve reliability [19]. Levin et al [20] report that reliability of volunteer generated data is improved by using multiple sources.

Hurricane Irma made landfall near Cudjoe Key, on September 10th, 2017 at 9:00 AM ET. Another landfall occurred on September 10th 3:35 PM at Marco Island near Naples [21]. This led to large scale evacuation of affected areas in the preceding days. Gasbuddy reported the data about the percentage of refueling stations out of fuel in major cities in Florida including Fort Myers- Naples, Miami-Fort Lauderdale, Tampa-St Petersburg, Orlando and Jacksonville from 9/6/2017 to 9/18/2017. Hurricane Florence, a slow-moving storm, damaged several regions in North and South Carolina in September 2018 and resulted in fuel shortages as high as 70% in some cities like Wilmington, North Carolina. The data from these hurricanes were used to parametrize our model. In addition, we use traffic data from the Florida Department of Transportation (FDOT) [22] and demographic data from the United States Census Bureau [23] in this work.

SIR Dynamics for Fuel Shortages

In the SIR model, schematically shown in FIG 1 (a), we treat the percentage of refueling stations without gasoline as "infected (I)", percentage of refueling stations with gasoline that are prone to running out of gasoline as "susceptible (S)" and percentage filled with gasoline after running out of fuel as "recovered (R)". The recovered refueling stations do not get re-infected (experience fuel shortage) in this case as the model and the on-ground situation represents a short-term outbreak. In terms of differential equations, the dynamic model for the SIR is:

$$\frac{dS}{dt} = -\beta S(t)I(t) \qquad \textit{Eq. 1}$$

$$\frac{dI}{dt} = \beta S(t)I(t) - \gamma I(t) \qquad \textit{Eq. 2}$$

$$\frac{dR}{dt} = \gamma I(t) \qquad \textit{Eq. 3}$$

The parameters β and γ represent the transmission rate per capita and recovery rate, which in the current context represent the rate at which the susceptible refueling stations are emptying and the empty gas stations are resupplied respectively. The quantity $\beta S(0)/\gamma$ is a threshold quantity known as a basic reproduction number (R_0). Here, we define it as the % of refueling stations without fuel in a region, because of 1% stations going out of fuel.

We use the crowdsourced data from the Gasbuddy website in conjunction with the Unscented Kalman Filter (UKF) to estimate the β and γ parameters. The Kalman Filter [24, 25], developed in the early 1960's, is an effective technique designed to estimate the parameters with measurement correction from empirical data. One of the earliest usages of the Kalman Filter was in the Apollo program [26], and it has seen widespread use in applications such as spacecraft reentry [27] and autonomous navigation through obstacle environments [28], as well as a diverse array of other engineering and epidemiological applications [29-31]. The use of the Kalman Filter for this parameter estimation problem, as opposed to conventional curve fitting techniques, facilitates bounding of the dynamic parameters. The best fit constant values for β and γ from all possible values are then used to develop the time invariant

continuous SIR data which closely resemble the empirical data. Different variations of Kalman Filter algorithms, such as the Extended Kalman Filter (EKF) [32], Ensemble Kalman Filter (EnKF) [33, 34] , and Sigma Point or Unscented Kalman Filter (UKF) [35], have been developed and used for various applications in engineering and epidemiology [24-35]. While the classical Kalman filter provides optimal state and parameter estimation for linear systems subject to Gaussian white noise, the process equations for the SIR problem, shown in Eqs 4 and 5, are inherently nonlinear, and the process and measurement noise are not necessarily Gaussian. The EKF algorithm can address nonlinearity by using the nonlinear dynamics for state propagation along with linearized dynamics to propagate the error covariance; however, the EKF assumes a Gaussian noise model. The Sigma Point or Unscented Kalman Filter (UKF) can accommodate nonlinear dynamics and it is not constrained by the assumption of Gaussian white noise. Instead, the UKF characterizes the estimation error by propagating a set of sigma points through the nonlinear dynamics model. Therefore, the UKF is used in this work for the estimation of the SIR model parameters. These data are then used in the optimal control algorithm to estimate an optimal refueling strategy.

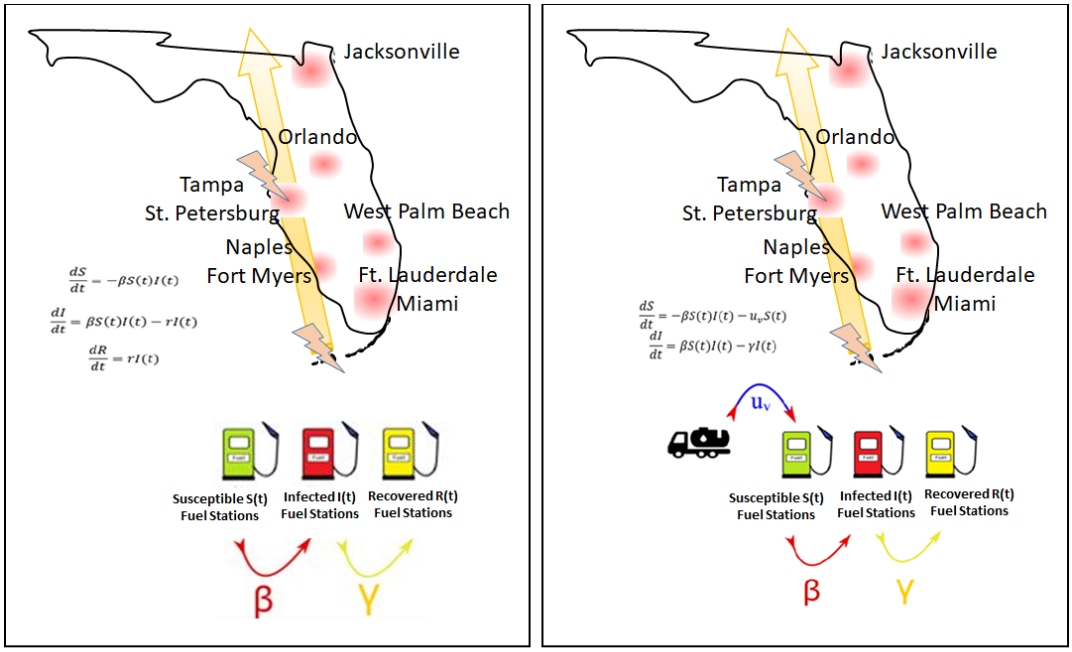

Figure 1.1(a). SIR dynamics model repurposed to study fuel shortages during hurricane evacuation (b) SIR dynamics model augmented to include vaccination rate as per capita rate of refueling, u_v.

By employing the fuel shortage data from Gasbuddy for the measurement update, we can simultaneously generate the synthetic data for the mechanistic SIR Model and estimate the parameters β and γ. The differential equations of the Fuel Shortage SIR model are then converted to discrete time form at different days, k, using the Euler Method. The state vector that is input into the UKF is defined as $X_k = [S_k, I_k, \beta_k, \gamma_k]^T$.

That is, the states are susceptible, infected, and recovered refueling stations and the parameters β and γ are the rates at which susceptible refueling stations are infected and infected refueling stations are recovered. The process equations, using the Euler method, for the UKF are then setup as shown below:

$$S_k = S_{k-1} + (-\beta_{k-1} S_{k-1} I_{k-1})dt \quad \textit{Eq. 4}$$

$$I_k = I_{k-1} + (\beta_{k-1} S_{k-1} I_{k-1} - \gamma_{k-1} I_{k-1})dt \quad \textit{Eq. 5}$$

$$\beta_k = \beta_{k-1} \quad \textit{Eq. 6}$$

$$\gamma_k = \gamma_{k-1} \quad \textit{Eq. 7}$$

. The output then takes the form of:

$$y_{1,k} = S_k \quad \textit{Eq. 8}$$

$$y_{2,k} = I_k \quad \textit{Eq. 9}$$

The Unscented Kalman Filter relies on the unscented transformation, which determines the statistics of an *L* dimensional random variable *x* through a nonlinear transformation *y=f(x)*. It is assumed that the state vector x has a known initial mean $\bar{x}$ and initial covariance P_0. The main goal of the UKF is to reduce the error in state estimation from a priori *(k-1)* value to a posteriori *(k)* value in each successive time interval *dt* for *N* time steps. Here, for Hurricane Irma, the entire time interval is 12 days with a time step of 0.25 days. For Hurricane Florence, more refined data were available, so we used a time step of 1 hour for the interval of 18 days. The statistics of the function y can then be determined using the procedures listed in the UKF pseudo-code as shown in Table 1.

In Step 1, we initialize the UKF by providing the initial values for state vector X_k for *t=0* days (k=1). We used a set of initial values of S_k and I_k from the Gasbuddy fuel shortage data for the first day. Initial values for β and γ were set to zero as they are to be determined

through the estimation process. The initial covariance, P_0 was set to the identity matrix with the same dimension as the state vector X_k.

The Q and R are the process and measurement noise covariance matrices in the estimation and update steps (Step 3 to Step 8) shown in Table 1. The cross-covariance matrices $P_k^{yy}\ and\ P_k^{xy}$ were initialized to R and the identity matrices respectively. The model update step entails propagating a set of 2L+1(where L is the number of states) sigma points through the nonlinear dynamics model (Eqs 4-7). The mean of the state estimate ($\hat{X}_{k|k-1}$) and the error covariance matrix ($P_{k|k-1}$) are then updated as a weighted combination of the propagated sigma points as shown in Step 4. The weighting matrices are computed as shown in Step 2. The measurement update is performed by first generating a set of measurements ($\psi_{k|k-1}^{i}$) by propagating the sigma points through the output equation (Step 5). The current measurement ($\hat{Y}_{k|k-1}$) is computed as a weighted combination of these propagated sigma points ($\psi_{k|k-1}^{i}$). The covariance and cross covariance estimation matrices are then updated as shown in Step 6, which in-turn are used to update the Kalman gain in Step 7. Finally, the mean of the state estimate and the error covariance matrix are updated in the last step. This process is then repeated until k=N. The states S_k and I_k are being updated at every time step, as are the states β and γ, defined by their relation to S_k and I_k in Eqs. 4 and 5. In this process we can estimate the transmission rate (β) and recovery rate (γ) for every time step from the data provided by Gasbuddy.

Table 1.1. Unscented-Kalman Filter estimation process

Step	Equation	Comment
1. Initialization	$X_0 = E[X_{k=1}]$, $\hat{X}_0 = E(\hat{X}_{k=1})$, $P_0 = E\left[(X_{k=1} - \hat{X}_{k=1})(X_{k=1} - \hat{X}_{k=1})^T\right]$ $Q = w_1 = [[1e1\ 1e1\ 1e2\ 1e2] * I_{n\times n}$, $R = [1e1\ 1e1] * I_{p\times p}$ $\left(P_k^{yy}\right)_{i=1} = R$ $\left(P_k^{xy}\right)_{i=1} = [0]_{L\times 2}$	k=1,2…, N. N= dimension of entire time interval divided in dt, time steps. i=1,2…, 2L+1. L= number of states in X_k.
2. Define Scaling Factor and compute weighting matrices	**Scaling factors** $\alpha = 1, \beta = 2$, $\kappa = 0$ $\lambda = \alpha^2(L + \kappa) - L, where\ L = size\ of\ X_k$ **Weighting Matrix** $W_m^1 = \frac{\lambda}{L+\lambda}$ $W_c^1 = \frac{\lambda}{L+\lambda} + (1 - \alpha^2 + \beta)$, $W_m^j = W_c^j = \frac{1}{[2(L+\lambda)]}\ for\ j = 2, \ldots, 2L + 1$	Assume Gaussian distribution

3. Generation of Sigma Points	$\sqrt{P_k} = Chol(P_k)$ $\chi_{k-1} = [X_{k-1} \quad X_{k-1} + \sqrt{(L+\lambda)P_{k-1}} \quad X_{k-1} - \sqrt{(L+\lambda)P_{k-1}}\,]$ **Use the known nonlinear system equation f(x) in Eq 4,5,6 and 7 to transform the sigma points into:** $\chi^i_{k\|k-1} = f(X^i_{k-1}) \quad for \;\; i = 1,2,\ldots,2L+1$	Where Chol is a MATLAB function for the Cholesky Decompositio n
4. Compute mean and covariance	$\hat{X}_{k\|k-1} = \sum_{i=1}^{2L+1} W^i_m \chi^i_{k\|k-1}$ $P_{k\|k-1} = \sum_{i=1}^{2L+1} W^i_c (X^i_{k\|k-1} - \hat{X}_{k\|k-1})(X^i_{k\|k-1} - \hat{X}_{k\|k-1})^T$	$\hat{X}_{k\|k-1}$ mean of predicted state
5. Generate Observation s	$\psi^i_{k\|k-1} = h(\chi^i_{k\|k-1})$ $\hat{Y}_{k\|k-1} = \sum_{i=1}^{2L+1} W^i_m \psi^i_{k\|k-1}$	$\hat{Y}_{k\|k-1}$ mean of predicted output
6. Covariance and cross covariance estimation	$P^{yy}_k = \sum_{i=1}^{2L+1} W^i_c \,(\psi^i_{k\|k-1} - \hat{Y}_{k\|k-1})(\psi^i_{k\|k-1} - \hat{Y}_{k\|k-1})^T$ $P^{xy}_k = \sum_{i=1}^{2L+1} W^i_c (X^i_{k\|k-1} - \hat{X}_{k\|k-1})(\psi^i_{k\|k-1} - \hat{Y}_{k\|k-1})^T$	

7. Compute Variable Kalman Gain matrix	$K_k = P_k^{xy}\left(P_k^{yy}\right)^{-1}$	Required for updating state prediction and reducing estimation error.
8. Update covariance and state matrices	$X_k = \hat{X}_{k\|k-1} + K_k\left(y_k - \hat{Y}_{k\|k-1}\right)$ $where\ y_k\ the\ output\ matrix\ \ for\ each\ time\ step\ k.$ $P_k = P_{k\|k-1} - K_k P_k^{yy} K_k^T$	Step 2-8 is repeated for each time step k.

Optimal Control Algorithm for the Refueling Strategy

The Unscented Kalman Filter provides estimates of the parameters β and γ, which are constant scalar values that can be used to develop a continuous time invariant dynamic model to characterize the fuel shortage as an infection. We now utilize this dynamic model to determine an optimal refueling strategy, which is modeled like a vaccination intervention, to mitigate the hurricane fuel shortage. The resulting control law is a bang-bang control policy. Bang-bang controllers [36] typically arise in minimum-time problems with constrained inputs, such as spacecraft maneuvers using thruster control [37, 38]. The result is a control input that corresponds to the maximum or minimum value with a finite number of switching times.

The SIR dynamics model is augmented to include vaccination [18] as shown below:

$$\frac{dS}{dt} = -\beta S(t)I(t) - u_v S(t) \qquad \textit{Eq. 10}$$

$$\frac{dI}{dt} = \beta S(t)I(t) - \gamma I(t) \qquad \textit{Eq. 11}$$

The term u_v in *Eq. 10* is the per-capita rate of refueling. Keeping congruency with our model parameters, u_v is the rate at which susceptible gas stations are prevented from being emptied out by external intervention in the form of additional fuel supply. The control variable u_v is bounded by practical constraints. The level of u_v that can be attained at any given time depends on the infrastructure that is in place to overcome fuel shortage problems such as the amount of gasoline in reserve in proximity to the area in question, the availability of transport vehicles etc. This resource constraint is addressed through the optimal control algorithm.

Let *r(t)* denote the total number of refueled fuel stations that were susceptible to becoming empty (infected) at time, *t*. The actual values of *S*, *I* and *r* will depend on the specific choice of the control u_v. Then, if $r_{max} \geq 0$ is fixed, u_v needs to be determined for the augmented SIR model in *Eq 10* that minimizes the cost function *(J)* shown in Equation 12 below. Similar approaches have been used for the vaccination analogue for infectious disease modeling [18].

$$J = \int_{t0}^{T} \beta S(t)I(t)\ dt \qquad \textit{Eq. 12}$$

subject to $S(t_0) = S_0, I(t_0) = I_0\ , I(T) = I_{min}, r(T) = r_{max}, u_v(t) \in [0, u_{v,max}]$ for all $t \in [0, T]$. Where, I_{min} is a threshold constant chosen to indicate the end of the fuel shortage problem at some arbitrary final time T.

This optimal problem can be solved by applying Pontryagin's Maximum Principle (PMP) [39]. In its general sense, consider the following optimal control problem with isoperimetric constraints:

$$min\, J = \phi\big(T, x(T)\big) + \int_{t_0}^{T} L\,(t, x, u)\, dt \qquad \text{Eq. 13}$$

Such that

$$\begin{cases} \dot{x} = f(t, x, u), x(t_0) = x_0, u \in\ U, \\ \int_{t_0}^{T} L(t, x, u)dt = \int_{t0}^{T} \beta S(t) I(t)\ dt\,, (Integral\ cost\ Function) \\ subject\ to\ resource\ constraint \\ R = \int_{t_0}^{T} u_v S(t)\ dt\ \leq r_{max} (Resource\ Constraints) \\ \psi\big(T, x(T)\big) = 0\ (Terminal\ Contraint) \\ \{\phi_x + [\phi_x]^T \vartheta - \lambda(T)\}^T|_T\ dx(T) + \{\phi_T + \vartheta^T \psi_T + H\}|_T\ dT = 0 \\ (Transversality\ Conditions) \end{cases} \qquad \textit{Eq. 14}$$

where $x \in \mathbb{R}^n$ is the state vector, $u \in \mathbb{R}^m$ is the control vector, ψ is a vector function, and ϕ, L are scalar functions. r is constant vector and U is an admissible control region, with continuous partial derivatives w.r.t all its arguments [18].

From the optimal control problem above, the PMP states: if u*(t) is an optimal control with x*(t) being the optimal trajectory, there exists a non-trivial solution of vector functions λ (costate functions) and nontrivial vector constants $\lambda_1, \lambda_2\ and\ \vartheta$ such that the conditions discussed below are met:

$$\begin{cases} \dot{x} = f(t,x,u), \dot{\lambda} = -H_x^T(t,x,u,\lambda), \\ H(t,x,u^*,\lambda,\lambda_1,\lambda_2) \geq H(t,x,u,\lambda,\lambda_1,\lambda_2), \forall\ admissible\ u, \\ x(t_0) = x_0, \psi\big(T,x(T)\big) = 0, \\ H\big(T,x(T),u(T),\lambda(T),\lambda_1(T),\lambda_2(T)\big) = -[G_T^T(T,x(T),\vartheta)]^T, \\ \lambda(T) = G_{x(T)}^T(T,x(T),\vartheta), \\ \int_{t_0}^{T} L_1(t,x,u)dt = \int_{t0}^{T} \beta S(t)I(t)\ dt, \int_{t_0}^{T} R(t,x,u)dt\ \leq r_{max}, \\ \lambda_2^T\left(\int_{t_0}^{T} R(t,x,u)dt - r_{max}\right) = 0, \lambda_2 \geq 0, \end{cases} \qquad \textit{Eq. 15}$$

where $H(t,x,u,\lambda,\lambda_1,\lambda_2) = L(t,x,u) + \lambda^T(t)f(t,x,u) + \lambda_1 L_1(t,x,u) + \lambda_2^T R(t,x,u)$ is the Hamiltonian, and $G\big(T,x(T)\big) = \phi\big(T,x(T)\big) + \vartheta^T\psi(T,x(T))$.

If the system in Eq 15 is time-invariant, the Hamiltonian, H, is constant [17] such that:

$H(t,x,u,\lambda,\lambda_1,\lambda_2) = const, \forall t \in [t_0,T]$.

Optimal Refueling Strategy

The deterministic SIR model for refueling with limited resources can be modeled by the governing equations shown in *Eq. 11* with the addition of the resource constraint derivative:

$$\dot{r} = u_v S \qquad \textit{Eq. 16}$$

If we construct this problem as a maximization problem, then Pontryagin's Maximum Principle (PMP) can be used to develop the relationship:

$$H(t) = -\lambda\beta SI - \lambda_S\beta SI - \lambda_S u_v S + \lambda_I\beta SI - \lambda_I\gamma I + \lambda_r u_v S \qquad \textit{Eq. 17}$$

Where the costate equations are satisfied as follows:

$$\dot{\lambda_S} = -(\lambda_I - \lambda - \lambda_S)\beta I - (\lambda_r - \lambda_S)u_v \qquad \textit{Eq. 18}$$

$$\dot{\lambda_I} = -(\lambda_I - \lambda - \lambda_S)\beta I + \lambda_I\gamma$$

$$\dot{\lambda_z} = 0$$

For this problem, the terminal cost and terminal constraint is 0. Hence, the transversality conditions can be reduced to:

$$\underline{\lambda}^T(T)d\underline{x}(T) + H(T)dT = 0 \qquad \textit{Eq. 19}$$

Where $dx(t) = [0, dS(t), 0, 0]^T$ and $\underline{\lambda}^T(T) = [\lambda(T), 0, \lambda_I(T), \lambda_r(T)]$, as *I(T)* and *r(T)* are fixed (constant) but *S(T)* is variable. Applying the PMP to the system in Eq. 15

$$H(t, x, u_v^*, \lambda, \lambda_1, \lambda_2) \geq H(t, x, u_v, \lambda, \lambda_1, \lambda_2), \forall\ admissible\ u_v \qquad \textit{Eq. 20}$$

$$-\lambda_S u_v^* S + \lambda_r u_v^* S \geq\ -\lambda_S u_v S + \lambda_r u_v S$$

$$u_v^* S(\lambda_r - \lambda_S) \geq u_v S(\lambda_r - \lambda_S)$$

The optimal control then becomes bang-bang control [18] where the switching function is given by $(\lambda_r - \lambda_S = 0)$ and satisfies

$$u_v^* = \begin{cases} u_{v,max}, \lambda_r > \lambda_S \\ ?, \quad \lambda_r = \lambda_S \\ 0, \quad \lambda_r < \lambda_S \end{cases} \qquad \textit{Eq. 21}$$

Following the development in Ref [18], it can be shown that that the optimal control is purely bang-bang, and there is no singular component or discontinuity. If $\lambda_r = \lambda_S$ on some interval *B*, then $\dot{\lambda_S} = 0$ on *B*. Eq 18 then can be simplified to:

$$0 = -(\lambda_I - \lambda - \lambda_S)\beta I - (\lambda_r - \lambda_S)u_v, (\ let\ u_v = 0) \qquad \textit{Eq. 22}$$

$$\lambda_I = \lambda + \lambda_s$$

We can further postulate that $\dot{\lambda_I} = 0$ on *B*. Hence, by Eq 18 and Eq 22, it must follow that $\lambda_I = 0$. Therefore, $\lambda_S = -\lambda$ and then the only nonzero criteria for the variables on *B* is $(\lambda, \lambda_S, \lambda_I, \lambda_r) = (1, -1, 0, -1)$. Furthermore, by Eq 18 and 19, once u_v^* becomes singular, it must remain singular throughout the whole interval *B*. Since, $T \in B$, $(\lambda, \lambda_S, \lambda_I, \lambda_r) = (1, -1, 0, -1)$ has to satisfy the transversality condition that $\lambda_S(T) = 0$ shown in *Eq. 18*. We

can further postulate that, since the boundary condition posed by the transversality condition is not met, the optimal control is purely bang-bang control. Now we examine the time at which the optimal control switches from 0 to $u_{v,max}$. Let the switch time be at t_s [18]. Then the Hamiltonian, H, at switching time, t_s can be written as follows:

$$H(t_s) = -\dot{\lambda}_I(t_s)I(t_s) = -\dot{\lambda}_S(t_s)S(t_s) - \lambda_I(t_s)\gamma I(t_s) = 0 \qquad \textit{Eq. 23}$$

By substituting $\dot{\lambda}_I(t_s) = 0$ into *Eq. 18* gives

$$(\lambda_S(t_s) + \lambda)\beta S(t_s) = \lambda_I(t_s)(\beta S(t_s) - \gamma) \qquad \textit{Eq. 24}$$

Considering the relations in *Eqs. 21* and *23*, the pure bang-bang optimal control is defined:

$$\lambda_I(t_s) > 0 \; when \; \dot{\lambda}_S(t_s) < 0 \rightarrow \left(0 \rightarrow u_{v,max}\right) \qquad \textit{Eq. 25}$$

$$\lambda_I(t_s) < 0 \; when \; \dot{\lambda}_S(t_s) > 0 \rightarrow \left(u_{v,max} \rightarrow 0\right)$$

$$\lambda_I(t_s) = 0 \; when \; \dot{\lambda}_S(t_s) = 0 \rightarrow (no \; switch \; occurs)$$

Since $\lambda_S(t_s) = \lambda_r = const., \lambda_S(t_s) + \lambda$ is either always positive, always negative or always zero. Suppose $\lambda_S(t_s) + \lambda = 0$. Then, by Eq. 24, either $\lambda_I(t_s) = 0 \; or \; S(t_s) = \frac{\gamma}{\beta}$. According to *Eq.25*, if $\lambda_I(t_s) = 0$, then no switching occurs.

Therefore, if $S(t_s) = \frac{\gamma}{\beta}$ then the optimal control has only one switch and this switching occurs when I(t) is maximum, since S(t) is a monotonically decreasing function of time [18]. So, the possible control switches are:

$$u_v^* = \begin{cases} u_{v,max}, t \in [0, t_s) \\ 0, \quad t \in [t_s, T] \end{cases} \qquad \textit{Eq. 26}$$

We consider $\lambda_S(t_s) + \lambda > 0$. By using the relations derived in Eq 24 and Eq 25 it follows that:

$$(i)\ \lambda_I(t_s) > 0\ and\ S(t_s) > \frac{\gamma}{\beta}\ \ or \qquad \textit{Eq. 27}$$

$$(ii)\ \lambda_I(t_s) < 0\ and\ S(t_s) < \frac{\gamma}{\beta}$$

Thus, by tracking the value of S(t) we can develop an algorithm to switch the control and determine the switching time analytically. In this SIR model for fuel shortage, the switching time, t_s, refers to the time when one should supply extra fuel to the operating fuel stations (susceptible at time t), to keep them operational in order to optimally control the fuel shortage epidemic to favorable levels.

The term u_v is the vaccination control for the SIR dynamic system. In our model we treat u_v as the percentage of operational fuel stations, S(t), that is being replenished to avoid additional fuel stations to go out of fuel. This is different from the recovery rate (γ) which is the rate at which non-operational fuel stations, I(t), are being replenished to become operational again. The optimal refueling rate per capita, u_v, is targeted at the susceptible compartment (S(t)) of the dynamic system. This has no effect on the recovery rate, γ.

The control is applied at $u_{v,max}$ from t=0 to a switching time, t_s to optimally reduce I(t), such that the basic reproduction number (R0) corresponding to the fuel shortage is less than 1, thereby mitigating the epidemic. The model suggests a combination of $u_{v,max}$ and t_s to achieve this objective. This approach helps to introduce optimal refueling control earlier in the evacuation period before the hurricane landfall and can determine the extra amount of reserve fuel required and the time period in which refueling is most effective.

RESULTS AND DISCUSSION

Parameter Estimation

The empirical data from the Gasbuddy crowdsourced platform are utilized to parameterize the models discussed above. The Unscented Kalman Filter is used to estimate the state variables and epidemic parameters (β, γ, R_0) based on these data. FIG 2 (a) shows the fuel shortage data for the 2017 Hurricane Irma and FIG 2(b) shows the similar data for the 2018 Hurricane Florence, which affected North Carolina. The plots indicate fuel shortages of up to 66% in South Florida during Hurricane Irma and similar shortages close to 70% in Wilmington, North Carolina during Hurricane Florence.

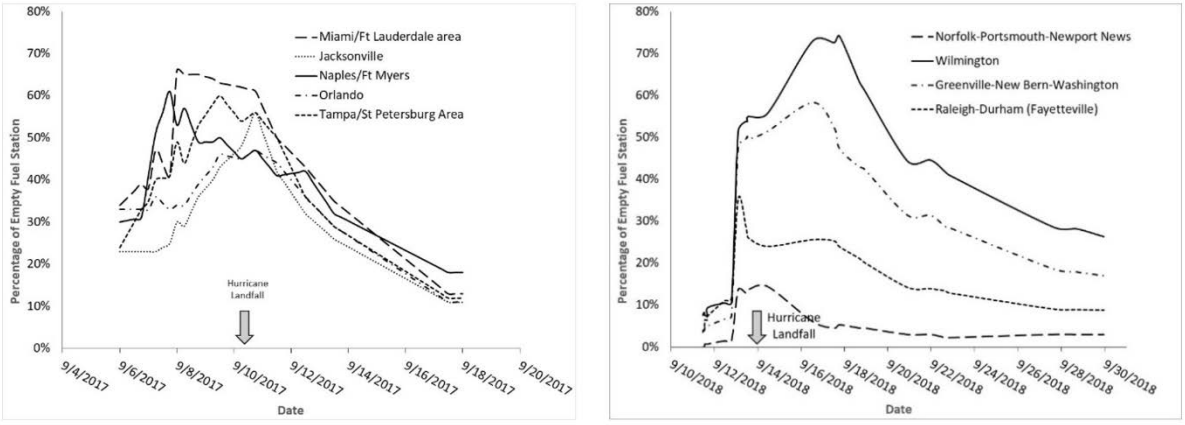

(a) (b)

Figure 1.2(a) The Fuel shortage data from 2017 Hurricane Irma, (b) Similar data for 2018 Hurricane Florence.

FIG 3(a) shows the variation of transmission rate per capita (β) and the recovery rate (γ) estimated using UKF for the Fort Myers-Naples metropolitan area where Hurricane Irma had a landfall on continental United States. Similar data for Wilmington affected by Hurricane Florence is shown in FIG 4 (a). While the fuel shortage data generally tend to peak ahead of

the landfall in preparation for evacuation, the fluctuations in fuel demand observed in FIG 2 cause the variations in the parameter estimations for β and γ. Consider the variation of the β parameter; in both FIGs 3(a) and 4 (a) an initial peak is followed by a stabilization indicating the high demand for fuel as the evacuation is starting. Compared to the Fort Myers-Naples, Wilmington displayed higher values of β which is indicative of the fact that fuel shortages occurred at a faster rate in Wilmington during Hurricane Florence than in Fort Myers-Naples during Hurricane Irma. The γ rate shows a gradual increase after the hurricane is passed, indicating the progress of the recovery.

We require a constant parameter SIR dynamical system described by equations 1 and 2, for the implementation of the optimal control refueling strategy. For this purpose, the mechanistic data produced using all combinations of the β and γ values, estimated by the UKF were compared with the empirical data to evaluate the mean square error. The best fit β and γ values are marked in FIG 3(a) and 4(a) for the two cases. FIG 3(b) shows the empirical fuel shortage data and the estimated continuous data with the constant β and γ values for Naples-Fort Myers. A similar plot for Wilmington during Hurricane Florence is shown in FIG 4(b). In both cases, we can observe that the estimated data for the continuous time invariant SIR model show close resemblance to the empirical fuel shortage data.

The continuous time invariant model SIR data for the remaining cities affected by Hurricanes Irma and Florence were computed in a similar way. The best fit values of β, γ and the basic reproduction number (R0) for all of the cities are tabulated in Table 2. The UKF estimation of β and γ values were unique to each city. While the values of β vary depending on the impact of Hurricane evacuation in the different cities, the evolution of β follows a similar

trend for all cities as shown in FIG 5. The similarity of γ values for different cities is indicative of the similarity in the recovery period for the different cities affected by Hurricane Irma. In the case of Hurricane Florence the slow moving nature of the storm and the difference in the infrastructure, in the affected communities resulted in the variation in the recovery periods.

The Unscented Kalman Filter used here is effective in reducing the linearization error when finding the parameters that generate data from Eqs 4 and 5 while representing the empirical data. In addition, this approach is effective in estimating the dynamic parameters with limited data during early stages of an ongoing hurricane evacuation. Such on-the-fly analysis can help decision makers allocate limited resources during an ongoing disaster.

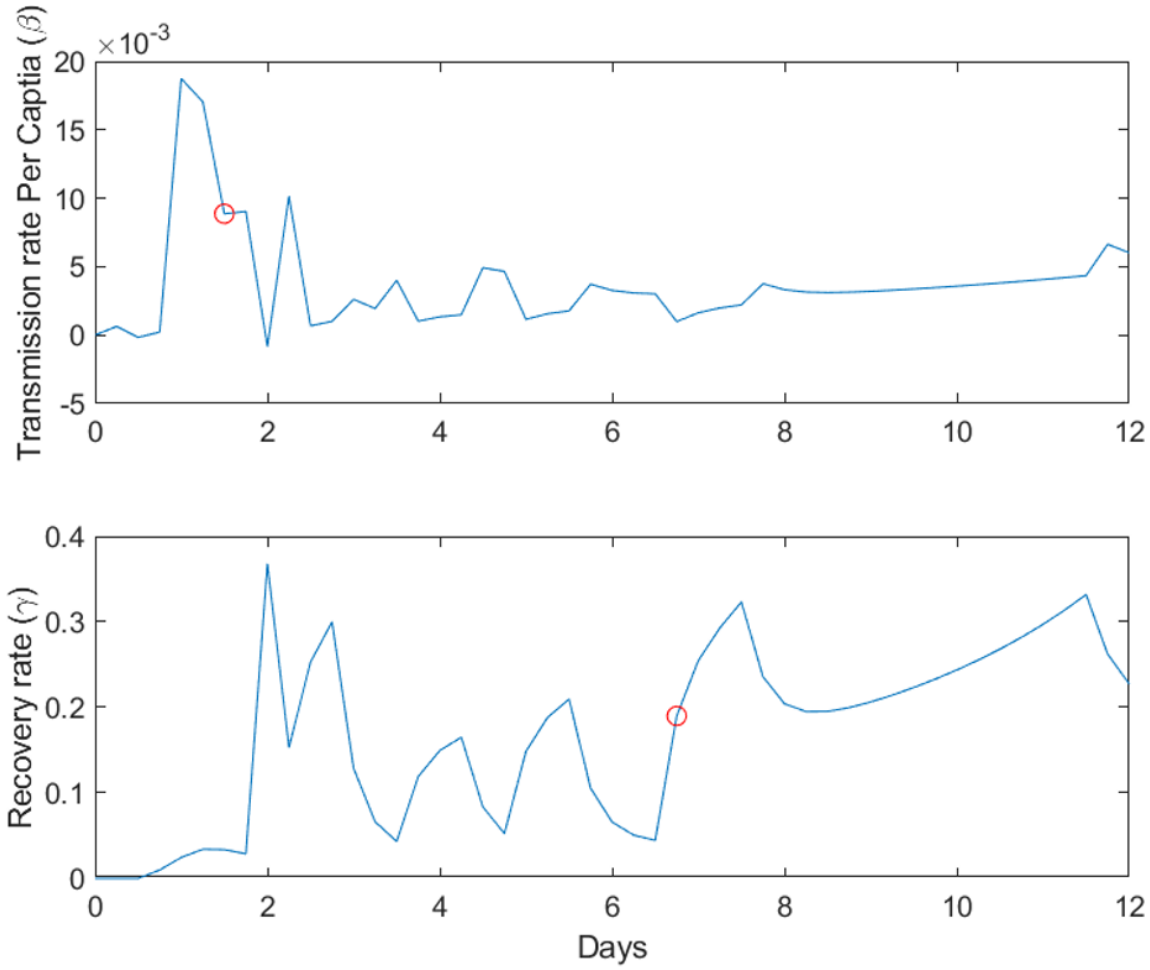
Transmission rate Per Captia (β)
$\times 10^{-3}$
20
15
10
5
0
-5
0
2
4
6
8
10
12
Recovery rate (γ)
0.4
0.3
0.2
0.1
0
0
2
4
6
8
10
12
Days

(a)

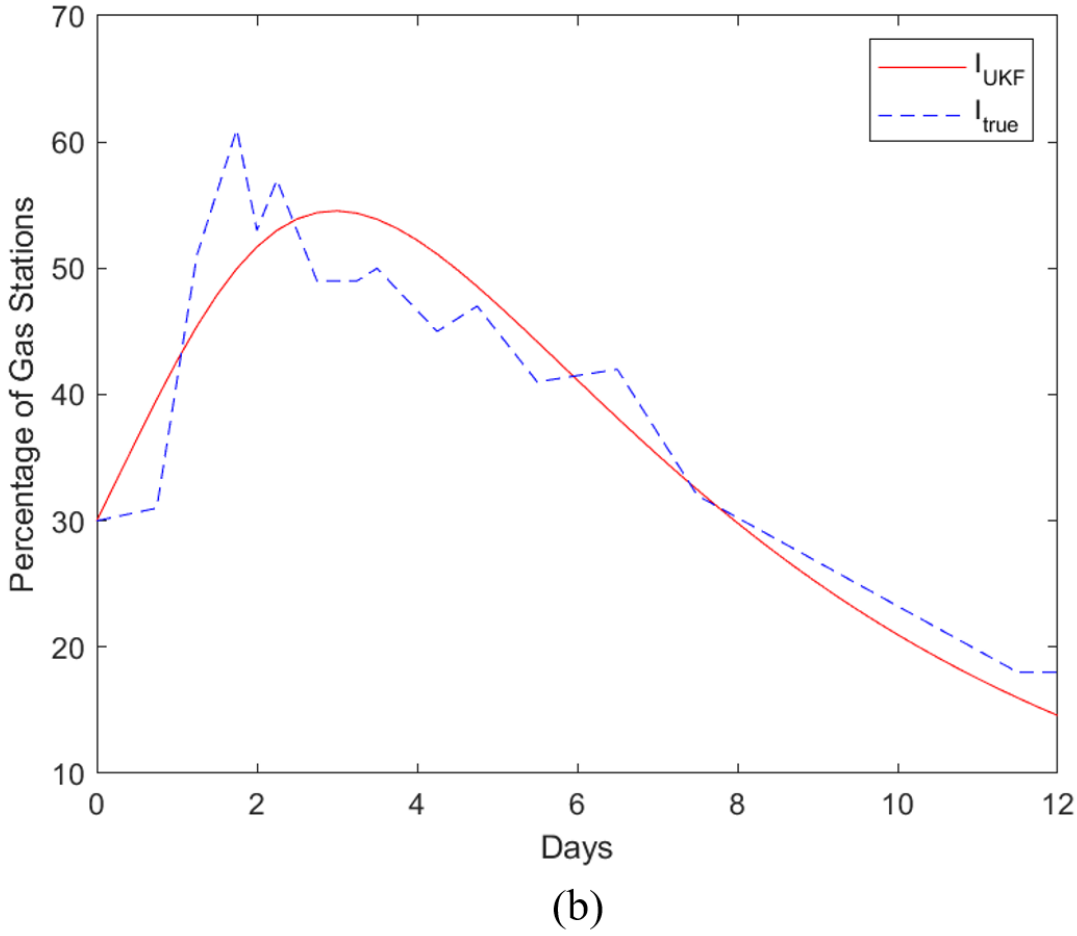

Figure 1.3(a). β and γ rates estimated from Gasbuddy data for each time step (dt) for Fort Myers-Naples during Hurricane Irma. The red circle represents the β and γ values used to plot I_{UKF} in 3(b). (b) Continuous time Invariant data of % empty fuel stations (I(t)). Computed data from the best fit β and γ constant parameters, and the empirical data is shown for Fort Myers-Naples during Hurricane Irma.

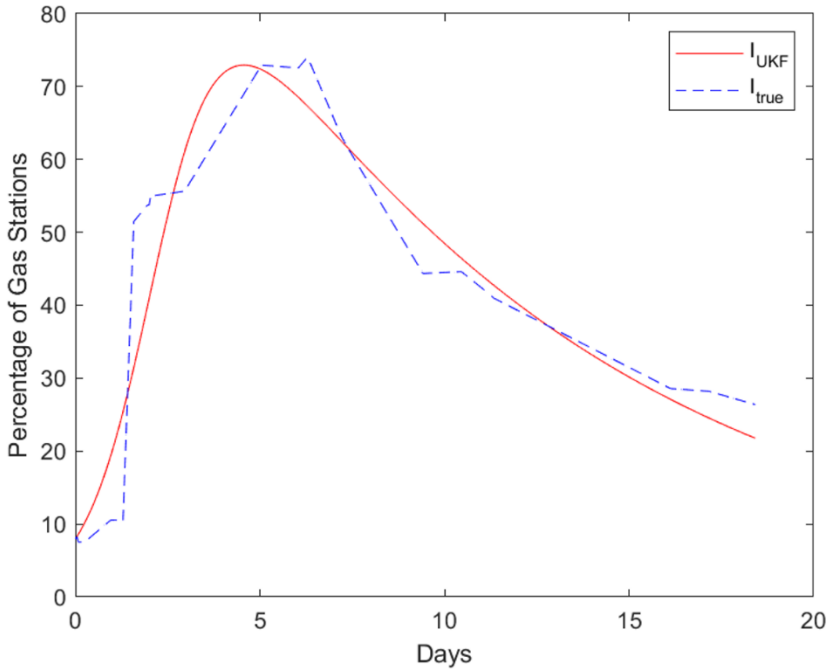

(b)

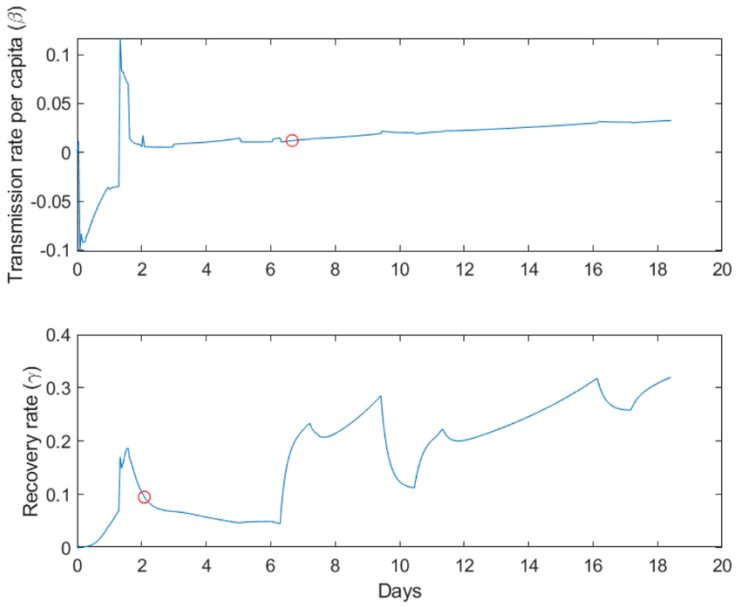

(a)

Figure 1.4(a). β and γ rates estimated from Gasbuddy data for each time step (dt) for Wilmington during Hurricane Florence. The red circle represents the β and γ values

used to plot I_{UKF} in 4(b). (b) Continuous time Invariant data of % empty fuel stations (I(t)). Computed data from the best fit β and γ constant parameters, and the empirical data is shown for Wilmington during Hurricane Irma

Table 1.2. β, γ and R_0 parameters and the number of fuel stations for the major cities affected by Hurricanes Irma and Florence.

Event	City/Area	Γ	β	R_0	No. Of Fuel Stations
Irma	Miami-Fort Lauderdale	0.1841	0.0111	3.98	1369
	Fort Myers-Naples	0.1901	0.0089	2.90	76
	Tampa-St Petersburg	0.1708	0.01	3.40	922
	Orlando	0.2214	0.006	1.57	810
	Jacksonville	0.2718	0.0097	1.61	453
Florence	Wilmington	0.0953	0.012	11.59	46
	Greenville-New Bern-Washington	0.1543	0.0143	8.91	130

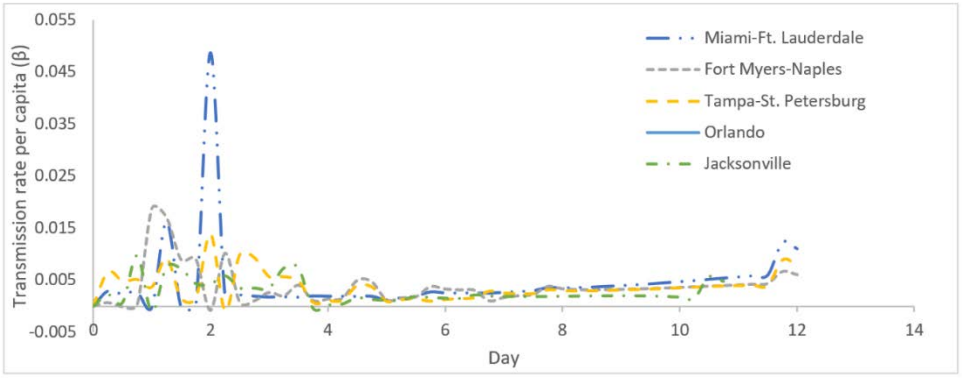

Figure 1.5. Transmission per capita rate (β) for the city/areas effected by hurricane Irma.

Optimal Refueling Strategy

We now present the results of the optimal refueling control algorithm for the SIR deterministic model formulated in the methods section. We utilize the constant values of transmission rate per capita (β) and the recovery rate (γ) estimated from the procedure outlined in the previous section. The continuous time invariant SIR data from these parameters closely resemble the empirical data and can be utilized directly in the optimal control algorithm. The results for the optimal refueling strategy are in the form of per capita rate of refueling ($u_{v,max}$) and the corresponding switching time (t_s), which control the fuel shortage epidemic, i.e. lower the basic reproduction number (R0), to non-epidemic levels as presented in *Eq. 27*. The per capita rate of refueling ($u_{v,max}$) corresponds to the fraction of susceptible fuel stations, S(t), that will be provided with extra refueling scheme at a given time. We vary this refueling rate ($u_{v,max}$) from 0 (no intervention) to 0.75 (75% refueling stations prevented from emptying), and determine the corresponding switching time (t_s) for the intervention to effectively reduce the fuel shortage below epidemic levels. When viewed

in totality, this analysis would provide a strategy to allocate limited resources to different affected regions from a hurricane.

FIG 6 (a), (b), (c) show the application of the refueling strategy to the Fort Myers-Naples region during Hurricane Irma. FIG 6(a) shows the percentage fuel stations that remain operational at any given time. The baseline is the curve corresponding to $u_v=0$ and is same as that in FIG 3(b). The baseline data generated using the UKF estimation process is the continuous time invariant representation of the empirical data and can be characterized by Eqs. 1 and 2. The remaining plots in 6(a) correspond to different refueling interventions. In these instances, the per capita rate of refueling ($u_{v,max}$), represents the fraction of gas stations that are prevented from becoming empty through external intervention till the switching time. The level of external intervention in terms of amount of fuel required changes every time step as the number of operational fuel stations (S(t)) changes. The application of this control strategy helps reduce the number of empty fuel stations, I(t), as shown in FIG 6 (b). FIG 6 (c) shows the application time and the switching time for the intervention. Here the per capita rate of refueling ($u_{v,max}$) is applied from the beginning of the observed time window and then switched to zero at the time designated by the condition in Eq 27. Note that application period for the refueling is well in advance of the hurricane landfall (Day 4 in this case). FIG 6 (b) and (c) show that the per capita refueling rate of 0.1 for 2.2 days reduces the peak fuel shortage from 55% to 48% and also moves the occurrence of peak shortage back by a day. When the $u_{v,max}=0.75$ is applied, the application period required is 0.5 days and it reduces the peak shortage to 37%. FIGs 7(a), (b) and (c) show similar data for Wilmington affected by Hurricane Florence. Similar trends for the effect of refueling strategy in reducing the

susceptible gas stations and in pulling back the peak fuel shortage time can be observed here as well. FIG 8 shows the evolution of infected or empty gas stations for other cities affected by Hurricane Irma, Miami-Ft Lauderdale, Tampa-St Petersburg, Orlando and Jacksonville. The β and γ values used to generate the baseline continuous time invariant SIR data corresponding to $u_v=0$ are shown in Table 2. The reduction in fuel shortages with different levels of intervention $u_{v,max}$ follows the same trend as that discussed earlier.

While increasing the refueling intervention levels reduces the number of empty refueling stations, there is a diminishing return when the intervention is increased beyond a certain level. FIG 9 (a) shows the variation in the peak value of empty fuel stations (I(t)) as the refueling rate ($u_{v,max}$) is increased from 0 to 1. The change of maximum I(t) is observed to be more in areas with higher rate of fuel shortage, i.e. high transmission rate per capita (β). For the Fort Myers-Naples area, with β=0.0089/day there is a gradual reduction in maximum I(t) as $u_{v,max}$ is increased. In the case of Wilmington, with β=0.012/day, there is a steeper change in maximum I(t) at low $u_{v,max.}$ In all the cases, there is a steady decrease in I(t) with the increase in the refueling rate; however, the rate of decrease is clearly higher for lower values of $u_{v,max}$. When this behavior is plotted as a bilinear relation as sown in FIG 9(b), the inflection point corresponds to the most effective refueling rate when there is a resource constraint.

An ongoing evacuation during a hurricane can be an evolving and dynamic problem. Residents in affected areas decide on the evacuation and preparation based on various factors like hurricane intensity, hurricane path and personal resources [40]. The ensuing fuel shortages can vary by location based on these factors. The approach presented here can help

decision makers with resource allocation during an ongoing emergency. In an ongoing evacuation scenario, the UKF parameter estimation can be used to estimate the β parameter for the affected regions even with limited data during the beginning of the fuel shortage. The γ parameter is related to recovery rate and can be estimated using the β estimate and an approximate recovery period based on historical data. This analysis for all the affected regions combined with the optimal refueling methodology discussed above can help assess the levels of fuel supply required to mitigate the fuel shortage crisis in the affected regions, and thereby assist decision makers in allocating limited resources in a dynamically evolving emergency.

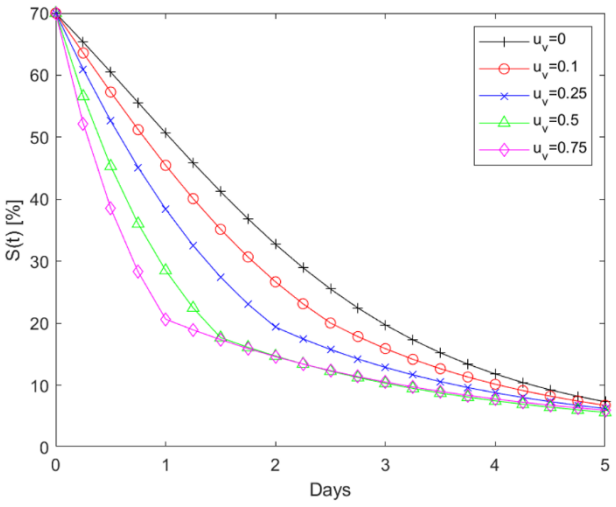

(a)

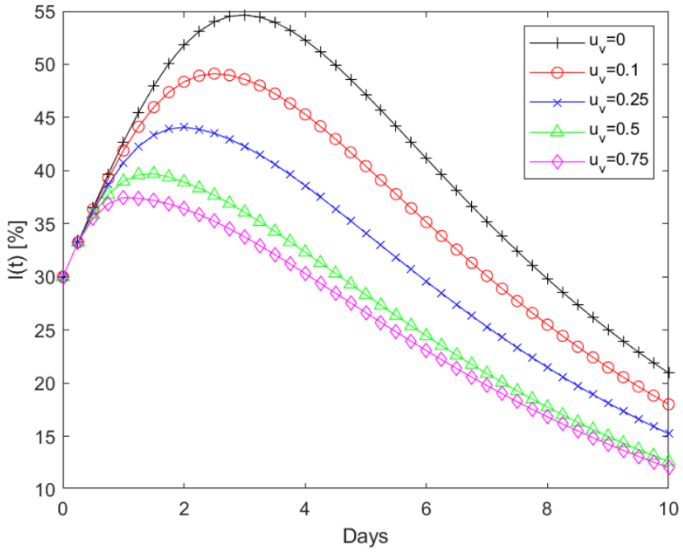

(b)

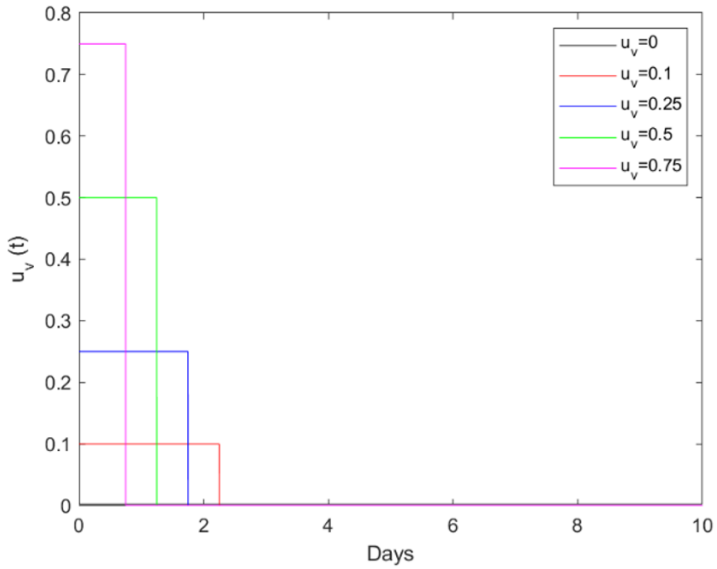

(c)

Figure 1.6 (a) Evolution of susceptible (operational) gas stations and the effect of refueling for Fort-Myers-Naples during Hurricane Irma. (b) Corresponding evolution of Infected or empty fuel stations. (c) The optimal application and switching time, t_s, for different refueling rates.

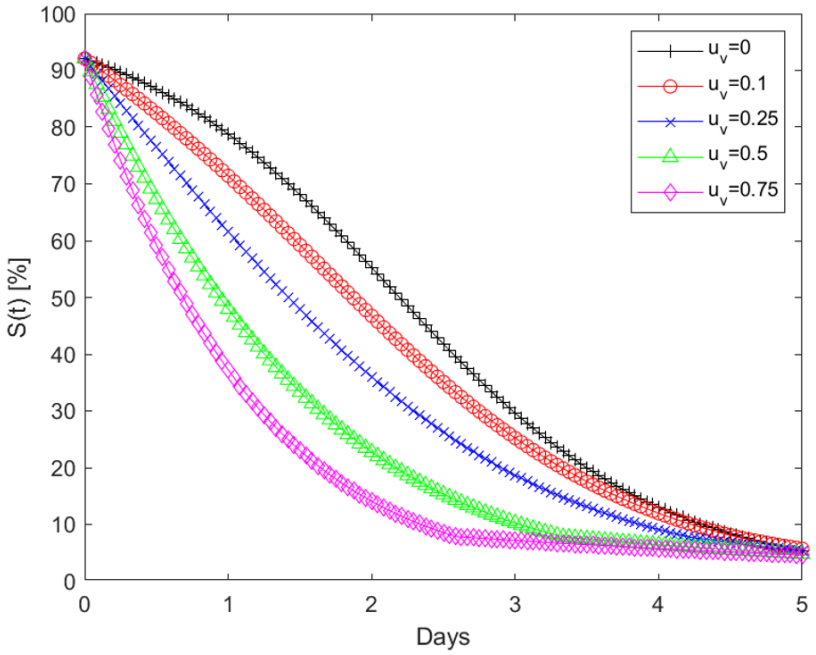
S(t) [%]
Days
u_v=0
u_v=0.1
u_v=0.25
u_v=0.5
u_v=0.75

(a)

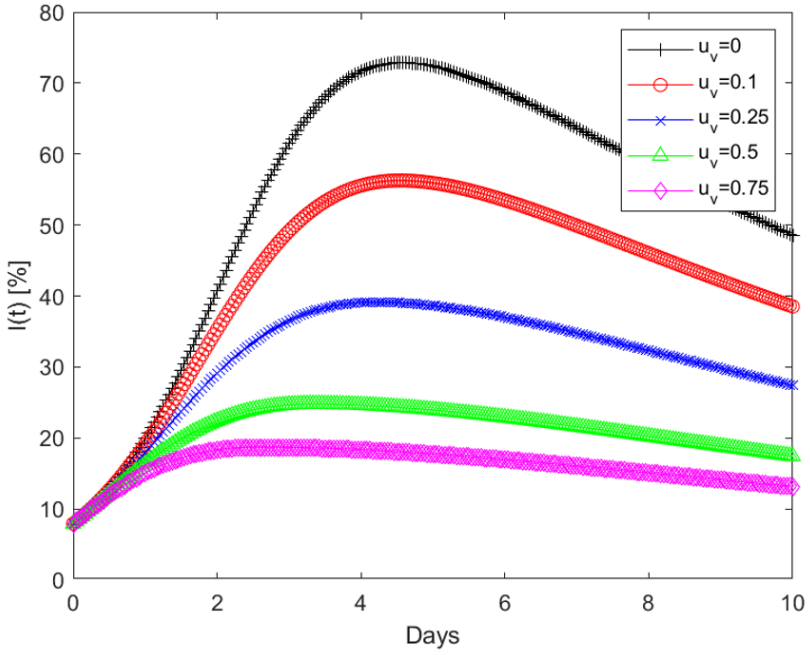
I(t) [%]
Days
u_v=0
u_v=0.1
u_v=0.25
u_v=0.5
u_v=0.75

(b)

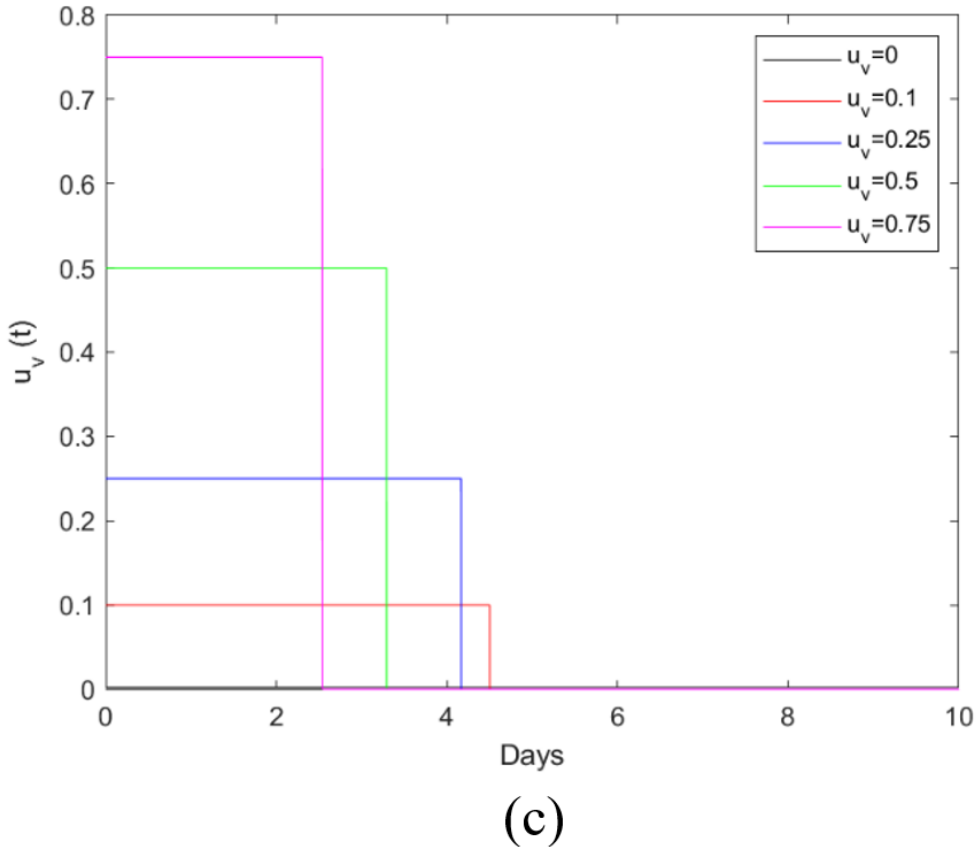

Figure 1.7 (a) Evolution of susceptible (operational) gas stations and the effect of refueling for Wilmington during Hurricane Florence. (b) Corresponding evolution of Infected or empty fuel stations. (c) The optimal application and switching time, t_s, for different refueling rates.

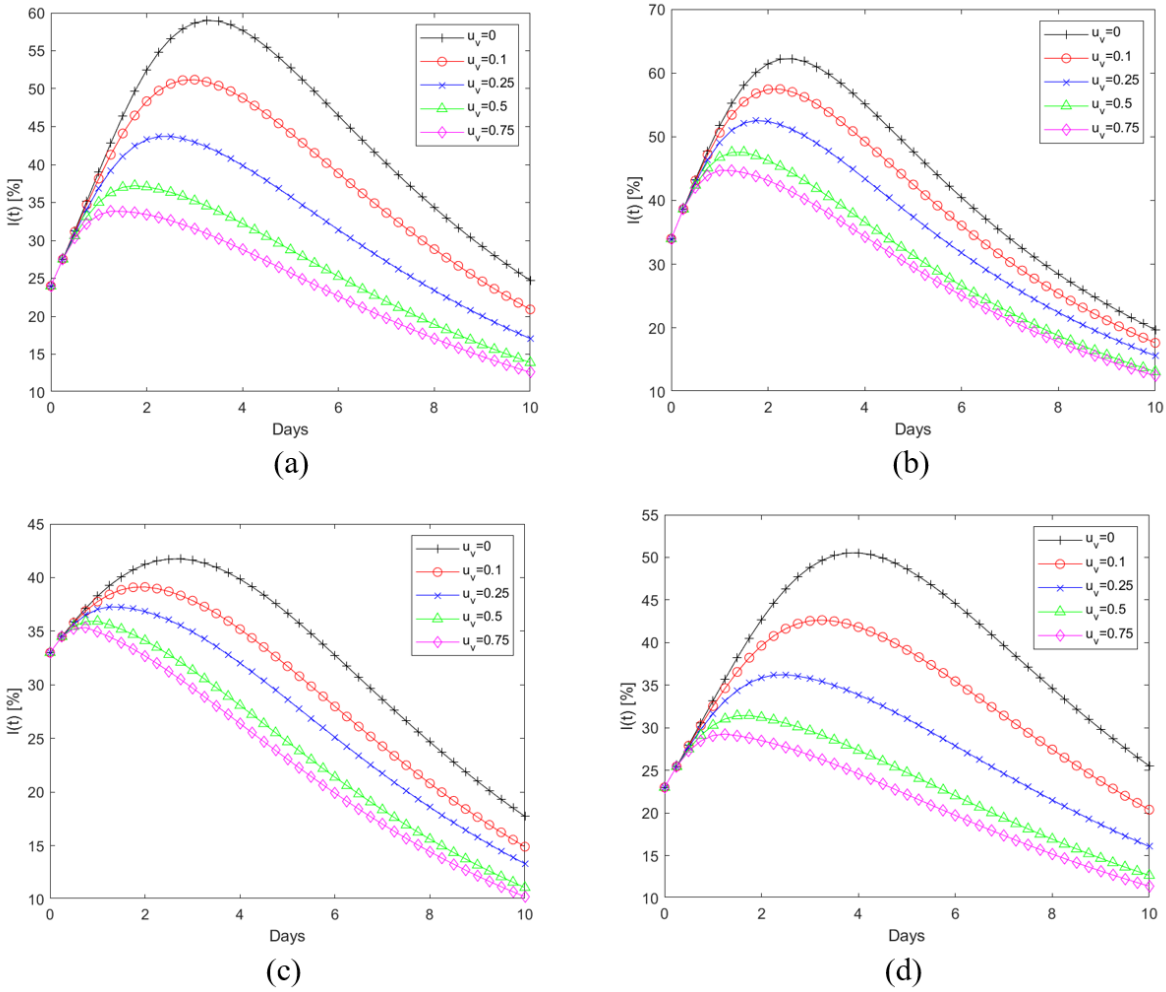

Figure 1.8. The evolution of empty gas stations and the effect of optimal refueling strategy on other cities affected by Hurricane Irma (a) Miami-Ft Lauderdale, (b) Tampa St Petersburg, (c) Orlando and (d) Jacksonville.

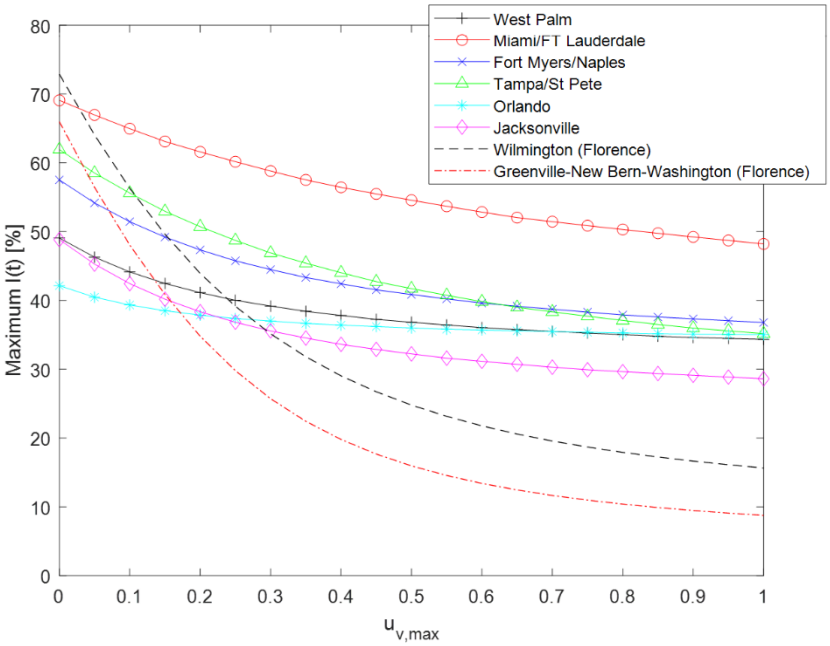

(a)

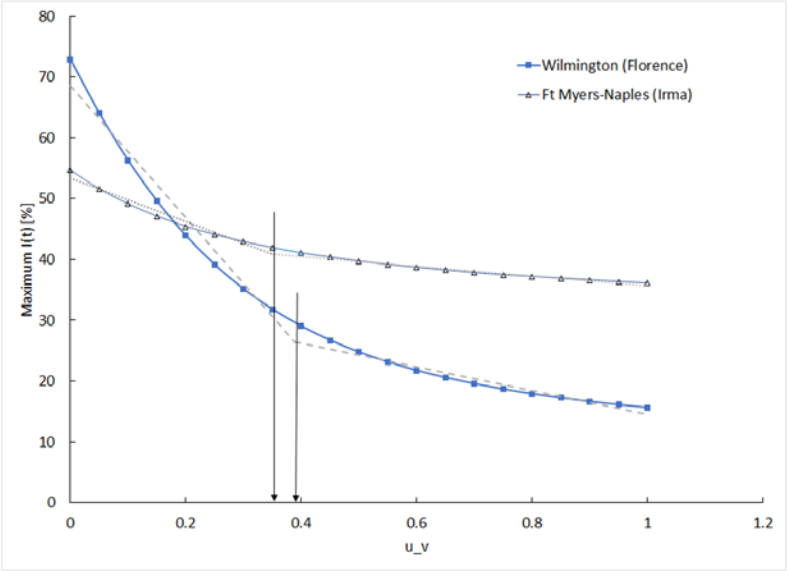

(b)

Figure 1.9 (a). Maximum number of empty fuel stations, I(t), for $u_{v,max}$ ranging from 0 to 1. (b). Bilinear Interpolation of Wilmington and Ft Myers-Naples to determine the optimal $u_{v,max}$. during Hurricanes Florence and Irma.

CONCLUSIONS

Fuel is a critical and limited resource during a natural disaster. Regional evacuations from major hurricanes can generate significant and often overwhelming fuel demand. In this study, for the first time we utilize a combination of social media crowdsourced data and epidemiological modeling techniques to address the problem of fuel shortages during hurricanes. We used the crowdsourced data from Gasbuddy to model the fuel shortage experienced during recent hurricanes as a contagion. The Unscented Kalman Filter was utilized to evaluate the dynamic parameters, transmission rate per capita (β) and recovery rate (γ), for multiple cities affected by Hurricanes Irma and Florence. An optimal refueling strategy was developed using Bang-Bang Control theory. The optimal control strategy provides useful insight into the control of a fuel shortage contagion using a vaccination analogue to the SIR model. The methodology can estimate the amount of fuel required at any given time to mitigate the epidemic fuel shortage in a given geographical region. This approach can be used to analyze fuel shortages during an ongoing evacuation and assist in resource allocation decisions.

CHAPTER 2. PREDICTIVE MODELING OF FUEL SHORTAGES DURING HURRICANE EVACUATION

(*This chapter is a journal paper in review*)

INTRODUCTION

Mass evacuations, particularly those at a state-wide level, place a significant burden on fuel supplies. The sudden and drastic increase in travel demand, compounded by disruptions to the supply chain and fuel hoarding from non-evacuees has been shown to cause localized fuel shortages during these large, single-event traffic movements [41]. Hurricane evacuees also tend to make longer, intercity trips to stay with friends and family, further increasing fuel demand [6]. During evacuations, fuel shortages can result in stranded cars and exacerbate traffic problems in an emergency [42]. During the 2017 Hurricane Irma evacuation, localized fuel shortages lasted several days and led to a cascade of problems. For example, the fuel shortages gave rise to unpredictable increases in fuel prices, placing additional barriers for evacuees living on low wage incomes. Fuel shortages also led to increased highway congestion near freeway off-ramps and service areas and resulted in evacuees detouring from designated routes, where less traffic was expected or planned for [3]. Even after the hurricane passed, fuel shortages continued to impede the recovery efforts, as utility crews struggled to fuel needed equipment necessary to restore power supply [3]. Understanding the characteristics of fuel shortages during a hurricane evacuation is crucial to the mitigation of these problems and reducing the casualties caused by an imminent hurricane.

While news reports have documented fuel shortages during past hurricanes, crowd-sourced data from the social media platform Gasbuddy [8] has quantified the shortages

during recent hurricanes, including Hurricane Irma. The analysis of crowdsourced data performed in this paper suggest characteristics of an epidemic for the evolution of fuel shortages. For example, as one gas station runs out of gas, drivers look to other stations in the vicinity to refuel. This places additional demand on neighboring gas stations, increasing the likelihood these stations will run out of fuel also. In this fashion, a fuel shortage at one location has "spread" to another. The goal of this paper is to develop a predictive model for estimating fuel shortages based on the Susceptible- Infected –Recovered (SIR) epidemic model using data collected from the 2017 Hurricane Irma evacuation. To limit the spread of fuel shortages, this paper identifies an effective "vaccination" strategy based on optimal control theory. To demonstrate the applicability of the proposed approach, the model is applied to a hypothetical storm making landfall in South Florida. The results of the analysis suggest that using the optimal control theory strategy to prioritize the refueling of gas stations, could lead to a 50 percent reduction in the number of depleted gas stations.

Literature Review and Background

Sociologists and computational scientists have long studied the spread of social phenomenon using epidemiological models with different contact and network parameters. Analyzing the connected social and behavioral events of a population as contagion leads to the study of these phenomena from a different perspective. For instance, contagious disease modelling has also been used to study social phenomena like, contagious adoption of health related behaviors [43], information spreading [44] and the spread of obesity through social ties [45]. Social contagion has also been characterized as a rumour spreading in social media [46] and spread of influential and public opinions in a population [47]. Several similar studies [48-50]

in various fields indicate the effectiveness of epidemiological models originally developed for disease studies in examining and predicting socially contagious phenomenon.

The 2017 evacuation from Hurricane Irma has been referred to as the largest evacuation in the history of the nation [51]. Approximately 6.5 million Floridians were placed under either mandatory or voluntary evacuation orders [3]. The overwhelming response to Hurricane Irma was driven by several factors that were unique to the storm: (1) Hurricane Irma had already devastated a number of Caribbean islands, including the U.S. Virgin Islands and Puerto Rico, resulting in several known deaths at the time [52]. (2) Hurricane Irma was the fifth strongest hurricane ever recorded in the Atlantic Ocean. (3) The storm path and "cone-of-uncertainty" threatened nearly the entire state of Florida. (4) Fluctuations in the storm's path indicated possible devastating storm surge to nearly all of Florida's coastal areas, where the majority of residents live. The overwhelming response to evacuation orders led to fuel shortages documented by Florida Department of Transportation [3]. FDOT provided five recommendations for limiting the impact of fuel shortages for future mass evacuation events:

(1) Provide law enforcement escorts for refueling vehicles
(2) Communicate the fuel availability during the event
(3) Provide regional waivers for the transportation of fuel across state lines
(4) Identify critical gas stations along state evacuation routes
(5) Provide traffic management plans for critical stations

Prior research into evacuation traffic as focused primarily on evacuation decision-making [40, 53-55] or estimating traffic volumes and congestion levels [56-60]. Wolshon [57] used ground-based detectors to report traffic volumes in Louisiana to estimate the vehicle response to Hurricane Katrina. Li et al. [58] used traffic count information collected from tollbooths to investigate evacuation response curves for Hurricane Irene from a single county in New Jersey. The research effort was later expanded to include historical travel time data and weigh-in-motion stations [59]. Spatial patterns were also investigated for Hurricane Sandy, although volumes were lower than for Hurricane Irene [60]. Prior attempts to model and predict the fuel shortages during an evacuation have used social media post to identified regions experiencing fuel shortages. The research then predicted where shortages were likely to occur [7]. In earlier work, Islam and co-workers (Islam, Namilae, Prazenica, & Liu, 2020) utilized Gasbuddy data to parametrize an SIR model using Unscented Kalman Filter (UKF). In this paper, that model is extended to correlate with traffic and survey data to predict the fuel shortages and suggest optimal control based remedial intervention strategies.

METHODOLOGY

The research methods seeks to pioneer a fuel shortage prediction model for application during evacuations by leveraging existing techniques found in epidemiological modeling. Broadly, this chapter describes the data sources, epidemic model development for fuel shortages, and the predictive analysis for evacuation traffic. The following sections detail these processes.

Data Sources

The Florida Department of Transportation's (FDOTs) Transportation Data and Analytics Office gathers roadway data from across the State of Florida. Real-time traffic information is provided during emergency such as hurricanes and wildfires. Traffic information, namely volume, speed, and vehicle classification, is collected hourly from telemetric monitoring stations located throughout the state. There are 255 data collection sites on Florida roadways at the time of this study, each providing bidirectional hourly counts and speeds. For the analysis of the Hurricane Irma evacuation, data were collected, cataloged, and processed for a 36-day period beginning August 27, 2017 and ending October 1, 2017.

The data pertaining to percentage of fuel stations out of gas, for this study, were acquired from Gasbuddy. Gasbuddy is an online database containing vital roadside information on more than 150,000 fuel stations. The website also provides real-time fuel price information to drivers through a designated mobile app created for both iOS and Android platforms [8]. Along with that, the website also enables existing drivers to report and review various refueling establishments throughout the United States. Gasbuddy played a crucial role during Hurricanes Irma and subsequent hurricanes by informing evacuees with real time information on fuel availability in different affected areas as they were evacuating. The crowd-sourced mobile app enabled drivers to report on fuel stations that were out of fuel in affected areas, thus contributing to driver awareness about fuel availability during the evacuation [19].

Epidemic Model for Fuel Shortages

A Susceptible Infected-Recovered (SIR) dynamic epidemic model [16] is utilized to model the fuel shortages with vaccination analogue used to represent the intervention efforts to address the fuel shortage. In a conventional disease epidemic, individuals are divided into the three compartments corresponding to susceptible, infected and recovered based on their infection status, and the dynamic parameters that describe this evolution are assessed by comparisons with empirical data.

A similar approach is used for refueling stations, wherein the percentage of refueling stations without gasoline is considered to be "infected (I)", percentage of refueling stations with gasoline that are prone to running out of gasoline is "susceptible (S)" and percentage filled with gasoline after running out of fuel as "recovered (R)". The recovered refueling stations do not get re-infected (experience fuel shortage) in this case as the model and the on-ground situation represents a short-term outbreak.

In terms of differential equations, the dynamic model for the SIR is:

$$\frac{dS}{dt} = -\beta S(t)I(t) - u_v S(t) \tag{1}$$

$$\frac{dI}{dt} = \beta S(t)I(t) - \gamma I(t) \tag{2}$$

The parameters β and γ represent the transmission rate per capita and recovery rate, which in the current context represent the rate at which the susceptible refueling stations are emptying and the empty gas stations are resupplied respectively. As in a conventional SIR model the mean infectious period, i.e. period in which most fuel stations are without fuel,

is$1/\gamma$.The quantity $\beta S(0)/\gamma$ is a threshold quantity known as a basic reproduction number (R_0). This is defined as the percentage of refueling stations without fuel in a region, because of 1 percent of stations going out of fuel. The R_0 value determines whether there is an epidemic taking place or not. If $R_0 < 1$, the epidemic dies out, while $R_0 > 1$ results in an epidemic [16, 18]. The term u_v is the per capita rate of refueling. Keeping congruency with our model parameters, u_v is the rate at which susceptible gas stations are prevented from being emptied out every day by external intervention that provides extra amounts of gas supply. This external intervention, in the form of additional fuel supply, can be provided by a governing agency or a private company. The level of u_v that can be attained at any given time depends on the infrastructure and planning that is in place to address the problem. For example, the gasoline reserves in proximity, the availability of transport vehicles and personnel etc. In extreme demand situations arising from large scale evacuations, the control resources can be considered to be limited. An optimal strategy to refuel is developed such that fuel shortage is kept at a favourable level throughout the interval being observed, subject to the limited fuel resources.

The refueling problem considered in this paper can be formulated as the following general optimal control problem:

Determine the optimal control $\underline{u}_*(t)$, $t_0 \le t < T$, where T is the unknown final time that minimizes the cost function

$$J = \int_{t_0}^{T} L(\underline{x}, \underline{u})\, dt \tag{3}$$

subject to the constraints:

$$\dot{\underline{x}} = \underline{f}\left(\underline{x},\underline{u}\right); \quad \underline{x}\left(t_0\right) = \underline{x}_0 \tag{4}$$

$$\underline{g}\left(\underline{u}\right) \le \underline{0} \tag{5}$$

Eq. (4) states that the state vector $\underline{x} \in R^n$ is dependent on the control input $\underline{u} \in R^m$ based on the system dynamics model, while Eq. (5) represents an inequality constraint on the control input. The classical approach is to append the dynamical system constraint (4) to the cost function as follows:

$$J' = \int_{t_0}^{T} \left\{ L\left(\underline{x},\underline{u}\right) + \underline{\lambda}^T \left(\underline{f}\left(\underline{x},\underline{u}\right) - \dot{\underline{x}} \right) \right\} dt = \int_{t_0}^{T} \left\{ H\left(\underline{x},\underline{u},\underline{\lambda}\right) - \underline{\lambda}^T \dot{\underline{x}} \right\} dt \tag{6}$$

where J' represents the augmented cost function, $\underline{\lambda} \in R^n$ is a vector of Lagrange multipliers, also known as the co-state vector, and the Hamiltonian H is defined as

$$H\left(\underline{x},\underline{u},\underline{\lambda}\right) = L\left(\underline{x},\underline{u}\right) + \underline{\lambda}^T \underline{f}\left(\underline{x},\underline{u}\right) \tag{7}$$

The classical solution to this optimal control problem for an unconstrained control input is given by the Euler-Lagrange equations [17]:

$$\dot{\underline{\lambda}} = -\frac{\partial H}{\partial \underline{x}} \quad \text{(Co-State Equation)} \tag{8}$$

$$\dot{\underline{x}} = \frac{\partial H}{\partial \underline{\lambda}} = \underline{f}\left(\underline{x},u\right) \quad \text{(State Equation)} \tag{9}$$

$$\frac{\partial H}{\partial u} = 0 \quad \text{(Stationarity Condition)} \tag{10}$$

$$\underline{\lambda}^T\left(T\right) d\underline{x}\left(T\right) + H\left(T\right) dT = 0 \quad \text{(Transversality Condition)} \tag{11}$$

For constrained inputs, the stationarity condition (Eq. 5) is generalized using Pontryagin's Minimum Principle, which states that the optimal control input corresponds to the control that minimizes the Hamiltonian when the state and co-state are fixed at their optimal values [61]:

$$H\left(\underline{x}_*, \underline{u}_*, \underline{\lambda}_*\right) \le H\left(\underline{x}_*, \underline{u}, \underline{\lambda}_*\right) \quad \forall\ \underline{u} \in U \tag{12}$$

where U represents the set of all admissible control inputs.

For the optimal refueling problem considered in this paper, the input constraint corresponds to the following resource constraint:

$$R = \int_{t_0}^{T} u_v(t) S(t)\, dt \le r_{\max} \tag{13}$$

A third state variable r is defined with the dynamics

$$\dot{r} = u_v S \tag{14}$$

The state vector is then defined as $\underline{x} = \begin{bmatrix} S & I & r \end{bmatrix}^T$, the control input is u_v, and the co-state vector is defined as $\underline{\lambda} = \begin{bmatrix} \lambda_S & \lambda_I & \lambda_r \end{bmatrix}^T$. The cost function to be minimized takes the form:

$$J = \int_{t_0}^{T} L\left(\underline{x}, u\right) dt = \int_{t_0}^{T} \beta S(t) I(t)\, dt \tag{15}$$

The final time is defined as the time when the number of infected states reaches a selected threshold, $I(T) = I_{\min}$, which would represent the end of the epidemic. The full system dynamics model $\dot{\underline{x}} = \underline{f}\left(\underline{x}, u\right)$ is given by

$$\begin{bmatrix} \dot{S} \\ \dot{I} \\ \dot{r} \end{bmatrix} = \begin{bmatrix} -\beta SI - u_v S \\ \beta SI - \gamma I \\ u_v S \end{bmatrix} \tag{16}$$

This corresponds to a nonlinear, time-invariant system. The control is constrained as follows:

$$0 \le u_v \le u_{v,\max} \tag{17}$$

The Hamiltonian takes the form:

$$H\left(\underline{x}, \underline{u}, \underline{\lambda}\right) = \beta SI - \lambda_S\left(\beta SI + u_v S\right) + \lambda_I\left(\beta SI - \gamma I\right) + \lambda_r u_v S \tag{18}$$

The Euler-Lagrange equations (Eq. 8) for the co-states are then given by

$$\begin{bmatrix} \dot{\lambda}_S \\ \dot{\lambda}_I \\ \dot{\lambda}_r \end{bmatrix} = \begin{bmatrix} \left(-1+\lambda_S-\lambda_I\right)\beta I + \left(\lambda_S-\lambda_r\right)u_v \\ \left(-1+\lambda_S-\lambda_I\right)\beta S + \lambda_I\gamma \\ 0 \end{bmatrix} \tag{19}$$

The optimal control input $u_{v,*}$ is determined using Pontryagin's Minimum Principle:

$$u_{v,*}\left(\lambda_{r,*}-\lambda_{S,*}\right) \le u_v\left(\lambda_{r,*}-\lambda_{S,*}\right) \quad \forall\ 0 \le u_v \le u_{v,\max} \tag{20}$$

This is equivalent to requiring that the optimal control minimize the left-hand side of the inequality. As a result, the optimal control policy corresponds to a bang-bang control law in which the control takes on either its maximum or minimum constrained value based on the sign of $\lambda_{r,*}-\lambda_{S,*}$, which is known as the switching function:

$$u_{v,*} = \begin{cases} 0 & \lambda_{r,*} > \lambda_{S,*} \\ ? & \lambda_{r,*} = \lambda_{S,*} \\ u_{v,\max} & \lambda_{r,*} < \lambda_{S,*} \end{cases} \tag{21}$$

Note that the optimal control is undefined when $\lambda_{r,*} = \lambda_{S,*}$; however, it can be shown, following a similar argument as presented in [18], that this condition does not occur for a finite period of time. Therefore, the optimal control policy is well-defined at all times and is purely bang-bang in nature.

In order to determine the optimal policy resulting from Eq. (21), it is necessary to compute the switching time(s) in the control law. First, since $I(T)$ and $r(T)$ are fixed, only $S(T)$ is free. As a result, the transversality boundary condition in Eq. (9) reduces to:

$$\lambda_S(T)\,dS(T) + H(T)\,dT = 0 \tag{22}$$

There is no direct relationship between $S(T)$ and T; therefore Eq. (20) results in $\lambda_S(T)=0$ and $H(T)=0$. Since the cost function and dynamics model are time-invariant, the Hamiltonian is also time-invariant. Therefore, $H(t)=0 \ \forall \ t\in[t_0,T]$.

Yang et al. [17] present a detailed proof, in the context of a parallel vaccination problem that first demonstrates that there is only a single switching time in the solution. Then, it is shown that starting with zero control and then switching to the maximum vaccination rate does not correspond to an optimal policy. As a result, the optimal solution corresponds to a policy in which the maximum vaccination rate should be applied from time t_0 until a single switching time t_s when the rate is reduced to zero. Applying this result to the refueling problem results in the following optimal refueling policy:

$$u_{v,*}=\begin{cases} 0 & t\in[t_0,t_s) \\ u_{v,\max} & t\in[t_s,T] \end{cases} \tag{23}$$

This corresponds to a policy in which fuel is supplied, starting at t_0, at the maximum rate until the switching time t_s, which is defined as the time when the number of susceptible gas stations is given by $S(t_s)=\frac{\gamma}{\beta}$. The final time T corresponds to the time at which the number of gas stations with fuel shortages (i.e., the number of infected states) is given by $I(T)=I_{\min}$.

The crowd sourced data from Gasbuddy platform for Hurricane Irma is used to parametrize the model. While there are several possible ways to estimate the parameters β and γ, an Unscented Kalman Filter (UKF) is utilized for this purpose in this paper. The Kalman Filter [24], developed in the early 1960's, is an effective method for estimating the parameters from empirical data with a measurement correction. The classical Kalman filter is

effective in providing the optimal state and parameter estimation for linear systems subject to a Gaussian noise. However, the model equations for the SIR problem (Eqs 1 and 2) are inherently nonlinear. The Unscented Kalman Filter characterizes the estimation error by propagating a set of sigma points through the nonlinear dynamics model; therefore, it is not limited by the assumption of Gaussian white noise [34]. It has been used for various applications in engineering and epidemiology [30, 31]. The detailed description of the parameter estimation using UKF for the SIR model is provided by Islam et al [62].

Predictive Analysis of Evacuation Traffic and Fuel Shortage

The above optimal control algorithm and the epidemic model are used for examining fuel shortage and for determining the optimal intervention control parameters. This model is parametrized with a prediction of fuel shortage data for a potential hurricane impacting south Florida. The step-by-step methodology for the model application is as follows:

(1) Analyze the cumulative traffic trends for evacuation during past hurricanes using transportation data. FDOT data from the Sunguide program for Hurricane Irma is used for this analysis.
(2) Analyze the fuel shortage trends for past hurricanes using the crowdsource data from the Gasbuddy app. The data form 2017 Hurricane Irma is used for this analysis
(3) Obtain the correlation between traffic and fuel shortage. For Hurricane Irma a near linear behaviour is observed. Note that the parameterization for steps 1-3 can improve significantly as data from historical and future hurricanes is used to develop the relation between evacuation and fuel shortage.

(4) The total evacuation traffic volume due to a hurricane impacting south Florida is estimated based on emergency response surveys as explained below. The evacuation traffic distribution in Step 1 is utilized to assess how this traffic is loaded over the evacuation period.

(5) The relation between traffic and fuel shortages from step 3 and the traffic estimate from step 4 are used to predict the fuel shortage distribution over the evacuation period. The optimal control methodology described in the above section is then applied to obtain the optimal refueling plan to mitigate the expected fuel shortage.

(6) A predictive model is then proposed where the UKF can be utilized to evaluate the SIR dynamic parameters from incoming fuel shortage during the initial stages of the hurricane. Due to the nature of the Ordinary Differential Equations (ODE) of SIR dynamics, only one of the parameters, infection rate (β) can be accurately estimated from the data collection of initial stages of the evacuation.

(7) The Basic Reproduction number (R0) value is then varied to produces predictive trends and the optimal refueling strategy is applied to these probable fuel shortage trends to demonstrate possible countermeasures.

The total evacuation traffic volume is predicted based on the state wide surveys conducted as a part of emergency planning. In response to the active hurricane seasons of 2004 and 2005, the Florida State legislature authorized the development of regional evacuation studies from across the state. Contracting with Florida's Regional Planning Councils, the Statewide Regional Evacuation Study Program (SRESP) was developed to support and update local government emergency management plans [54]. As part of the

SRESP, a series of surveys was conducted to better understand evacuation behavior and to facilitate improved behavioral assumptions for use in evacuating modeling and shelter planning. The behavior assumptions collected as part of this survey were: evacuation rate, out-of-county trips, type of refuge, percent of available vehicles, and evacuation timing. Surveys were conducted on 400 residents in each of Florida's 67 counties.

The results of the SRESP surveys were analyzed to estimate the auto-based evacuation in response to a Category 1 and Category 3 hurricane landfall in Broward and Miami-Dade county FL. The 2017 census data [63] was used to estimate the number of site-built and mobile homes in both regions. Then the SRESP survey results were used to estimate the evacuation participation rate, percent of vehicles used, and the number of available vehicles. Through the process outlined in SRESP, the "maximum probable" number of evacuating vehicles was estimated for the hypothetical storms [54]. This analysis suggest that 173,914 vehicles would likely be used in the evacuation of Miami Dade County in the event of a Category 1 hurricane landfall in the region. A total of 342,379 evacuating vehicles were estimated from the area in the event of a Category 3 storm.

Result and Discussions

The results linking traffic volume and fuel shortage for various population centers in Florida are presented first. The hourly counts of vehicles obtained from FDOT's SunGuide program are analyzed to obtain cumulative outgoing traffic count over the days impacted by Hurricane Irma. Irma made two landfalls, the first in Cujoe Key and the second on to US mainland at Marco Island near Naples on Sep 10 at 3:35 PM [64]. The second landfall is referenced in Figures 1(a)-1(d). The cumulative egress from Napes-Fort Myers metropolitan

area is shown as the dotted line in Figure 1. The evacuation out of this area started three to four days before the hurricane landfall and reached peak by Sep 9. The flat peak around the hurricane landfall period indicates the reduced traffic volume during the hours impacted by the hurricane. The solid line in Figure 2(b) shows the fuel shortage reported by Gasbuddy crowdsource platform in the form of percent refueling stations without fuel. The peak for the fuel shortage lags the peak evacuation traffic as can be expected. When faced with a threat of looming hurricane, people usually fill-up their vehicles in preparation for a potential evacuation, even if they eventually decide not to evacuate. As can be observed form Figure 1(b) up to 60 percent of the refueling stations in Naples- Fort Myers area were without gas as the evacuation traffic was peaking.

Figure 1(b) shows a similar plot for Tampa-St Petersburg metropolitan area. The plot shows similar trend as that of Naples, with respect to flat traffic peak around landfall and the period impacting this region. Fuel shortages of up to 60 percent can be observed lagging the peak of evacuation traffic for this region as well. Figure 1(c) shows similar data for Miami-Fort Lauderdale Metropolitan area. This is the largest metropolitan area in Florida with significantly higher population. While the trend is similar to that observed in Figures 1(a) and 1(b), there are fluctuations in both traffic peak and fuel peak. This can be attributed to the early uncertainty in the hurricane path. While the hurricane eventually made landfall close to Naples, early predictions indicated a possible landfall near Miami (NHC, 2017). This may have prompted early increase in evacuations which stabilized as the hurricane path was more certain. Figure 1(d) shows the similar plot for Jacksonville.

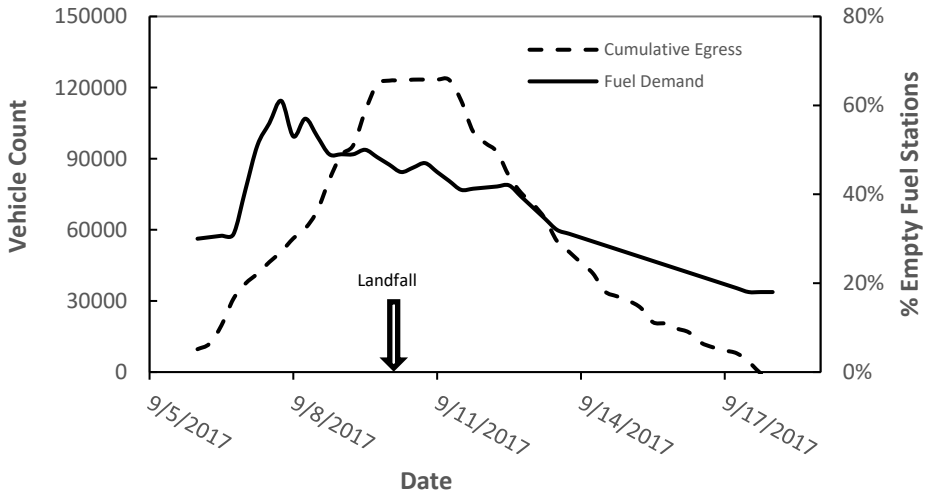
150000
120000
90000
60000
30000
0
80%
60%
40%
20%
0%
Vehicle Count
% Empty Fuel Stations
Cumulative Egress
Fuel Demand
Landfall
9/5/2017
9/8/2017
9/11/2017
9/14/2017
9/17/2017
Date

(a)

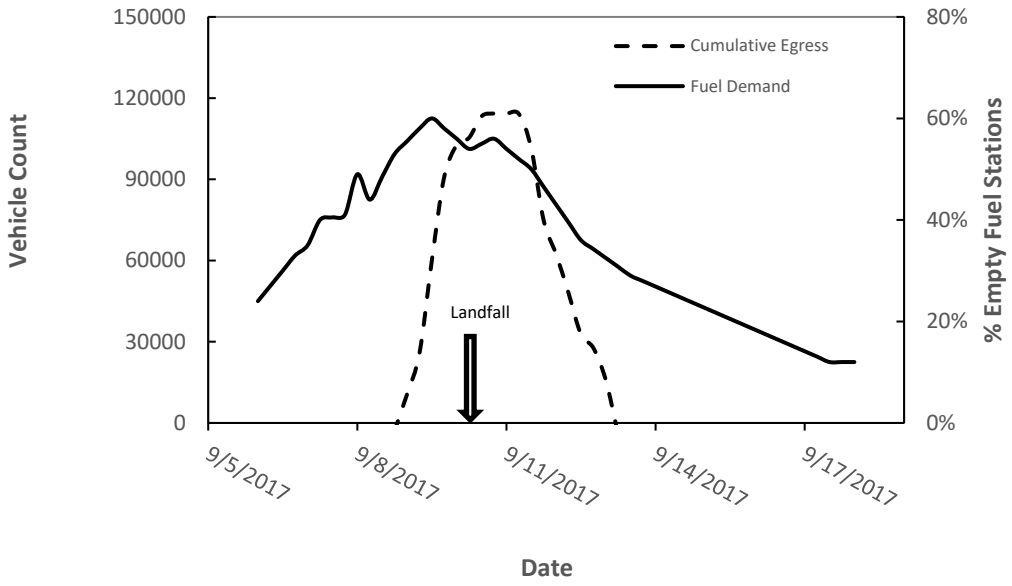
150000
120000
90000
60000
30000
0
80%
60%
40%
20%
0%
Vehicle Count
% Empty Fuel Stations
Cumulative Egress
Fuel Demand
Landfall
9/5/2017
9/8/2017
9/11/2017
9/14/2017
9/17/2017
Date

(b)

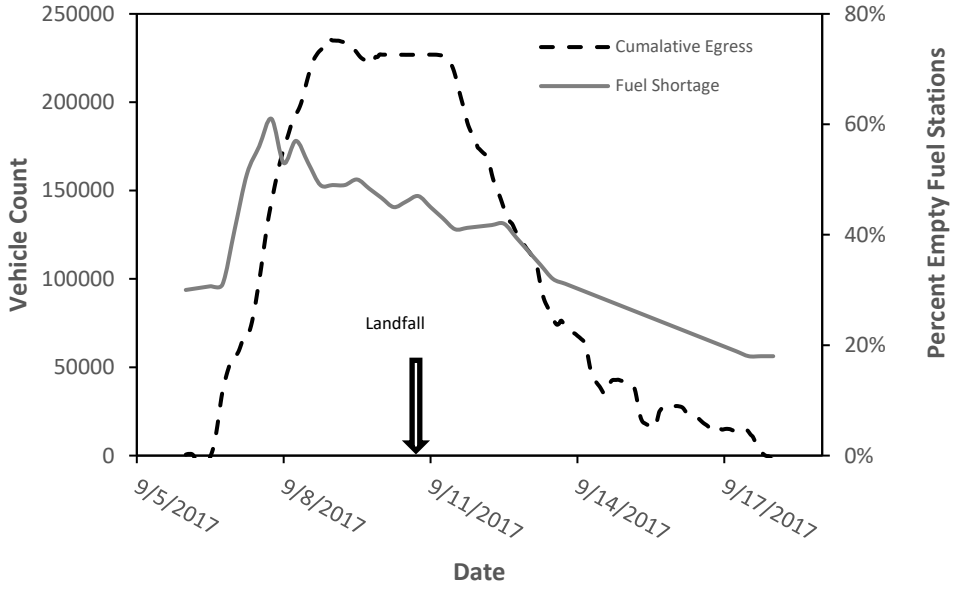

(c)

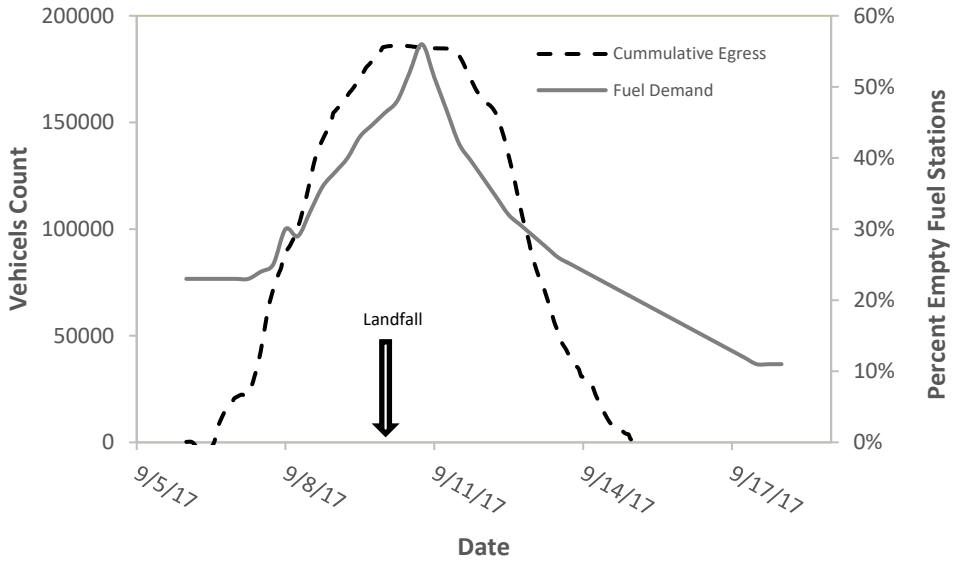

(d)

Figure 2.1 (a) Fuel shortage and cumulative egress for Naples, FL. (b) Fuel shortage and cumulative egress for Tampa, FL. (c) Fuel shortage and cumulative egress for Miami/Ft Lauderdale, FL. (d) Fuel shortage and cumulative egress for Jacksonville, FL

The data in the above figures 1(a) to 1(d) are used to obtain a correlation function between the evacuation traffic volume and fuel shortage. This correlation for Miami-Ft Lauderdale area is shown in Figure 2. Since there is a delay in the peaks of both fuel demand and cumulative egress the plot for fuel demand is shifted to match the peak value around the same time as the cumulative egress for all the city/area. This is done as it is hypothesized that there is a direct correlation between the occurrence of these peak values without taking the uncertainties of evacuation considered. Table 1 shows the time delay (ΔT), in days, that was observed for different city/areas in fuel demand and cumulative egress.

Table 2.1. Time Delay between peak fuel demand and peak cumulative egress for different cities.

City/Area	ΔT (Days)	I_{MAX}	Cum. $Egress_{MAX}$	No. of Fuel Stations
Ft Myers-Naples	3.25	0.61	123356	76
Tampa-St Petersburg	1.25	0.6	114312	922
Miami-Ft Lauderdale	1	0.66	234924	1545
West Palm Beach	0	0.56	36968	34
Jacksonville	0	0.56	185861	453

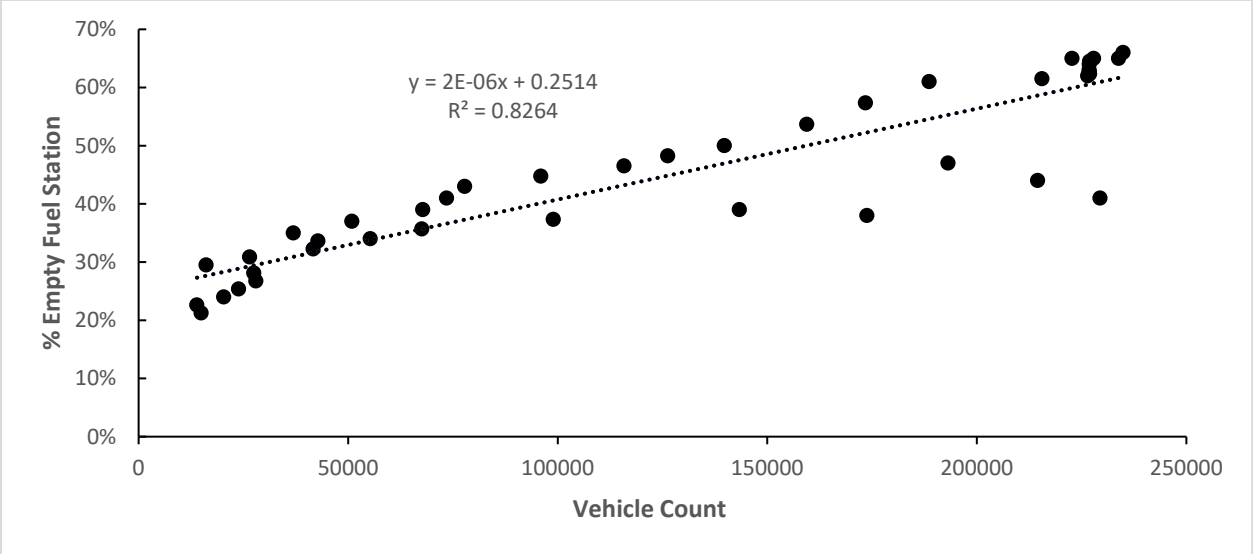

Figure 2.2 Relationship between fuel demand and cumulative egress for Miami-Ft Lauderdale.

Predictive Modelling and Optimal Control

Consider a hurricane that would make a direct impact on South Florida. In this section, the results of a predictive model for fuel shortages due to evacuation from such a hurricane are analyzed and an optimal intervention strategy is developed for such fuel shortages. The total traffic volume evacuating out of Miami-Dade County is estimated based on Statewide Regional Evacuation Study Program (SRESP) surveys [54]. The survey results on the likelihood of evacuation for residents in different surge protection zones are scaled to the population of metropolitan area and average vehicle availability for the households from US census to estimate the total evacuation numbers. Table 2 below provides the details of the calculation for a category 3 hurricane that would make landfall in Miami-Dade County. A similar estimate for Category 1 hurricane generates 173,914 vehicles evacuating Miami metropolitan area.

The total evacuation traffic is distributed across the evacuation period based on the traffic distribution during Hurricane Irma. A normalized aggregate traffic distribution, which is essentially a combination of the traffic data from Figures 1(a) to 1(d), is used for this purpose. The resulting fuel shortage due to the traffic volume is estimated using the regression coefficients in Table for Miami region. Figure 3 shows the estimate of fuel shortage. Both the prediction of the loading pattern and the fuel shortage prediction can improve significantly as data from additional historical and future hurricanes are used to develop the relation between evacuation and fuel shortage.

Table 2.2. Calculation of total evacuating vehicles for Miami-Dade County for a Category-3 hurricane. The sources for data are [54] and [63].

EVAC	HOUSE		EVAC RATE		VEH USE RATE		VEH/HH	EVAC VEH	
ZONE	BUILT	MOBILE	BUILT	MOBILE	BUILT	MOBILE		BUILT	MOBIL
Cat 1	56,046	871	65%	85%	80%	85%	1.5	43,716	944
Cat 2	80,323	1144	60%	80%	70%	75%	1.9	64,098	1,305
Cat 3	94,206	2346	60%	80%	70%	75%	1.9	75,177	2,675
Cat 4	175,122	1704	30%	75%	65%	70%	2.1	71,713	1,879
Cat 5	188,004	3084	15%	75%	65%	70%	2.1	38,494	3,401
Inland	422,067	7,039	5%	65%	75%	80%	2	31,656	7,321
								Total Vehicles = 342,379	

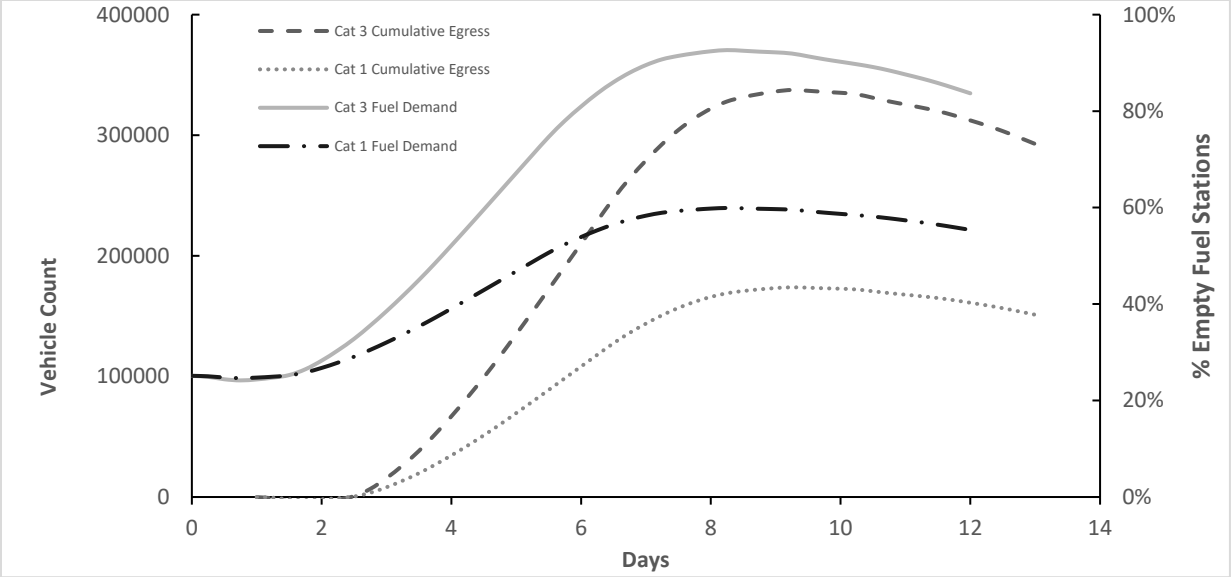

Figure 2.3 Prediction of cumulative egress and fuel shortage for: (a) Category 3 hurricane directly impacting Miami FL, and (b) Category 1 hurricane directly impacting Miami FL.

Once the predictive model is used to parameterize the fuel shortage data, the optimal refueling strategy approach is used for further analysis. An Unscented Kalman Filter (UKF) algorithm [34, 35] is used to estimate the transmission rate per capita (β) and the recovery rate (γ) of the predicted fuel shortage. The optimal refueling strategy is then used to determine the best scenario for mitigating the fuel shortage problem under a resource constraint. In Figure 3, equations 1 and 2 to are utilized to deterministically produce the time-invariant data of the SIR dynamics without intervention, i.e. using u_v=0. The epidemiological parameters corresponding to the transmission per capita rate and the recovery rate for the predicted category 3 and category 1 hurricanes are shown in Table 2. The use of UKF for parameter estimation is necessary as the evolution of infected gas stations (I(t)) from the

prediction model was time-variant, but the optimal refueling strategy developed in the methods section is based on a time-invariant, continuous-time non-linear dynamic system.

Figure 5(a) and 5(b) show the change in percentage of empty fuel stations or I (t) as the optimal refueling strategy is applied. With u_v=0 (i.e. no intervention), for a category 3 hurricane making a direct hit on Miami, the model predicts that the fuel shortages will be more than 80 percent. If the resources are used to provide relief to 75 percent of the gas stations at any given time (i.e. u_v=0.75), the fuel shortages would be reduced to 29 percent. Figure 6(a) shows that the optimal switching time for the bang-bang controller with u_v=0.75 is 3 days. This implies that the infectious behaviour of fuel shortage can be mitigated by providing relief to 75 percent of operating refueling stations for the first 3 days after the start of evacuation. This essentially means that the R0 parameter described earlier is less than 1 under these conditions, *i.e.* 1 percent gas stations going out of fuel does not cascade into fuel shortage beyond this 1 percent. When R0 is higher than 1, like with (u_v=0), 1 percent gas stations going out of fuel leads to an additional R0 percent refueling stations going out of fuel due to the infectious behaviour. Figure 5 and 6 show how the switching function (t_s) and the level of intervention (u_v) can be varied to optimally control the problem and mitigate the infectious behaviour.

TABLE 2.3 Results of parameter estimation using the UKF for the fuel shortage prediction

Parameter	**Category 1**	**Category 3**
Transmission rate per capita (β)	0.0028/day	0.0043/day
Recovery rate (γ)	0.0453/day	0.0105/day

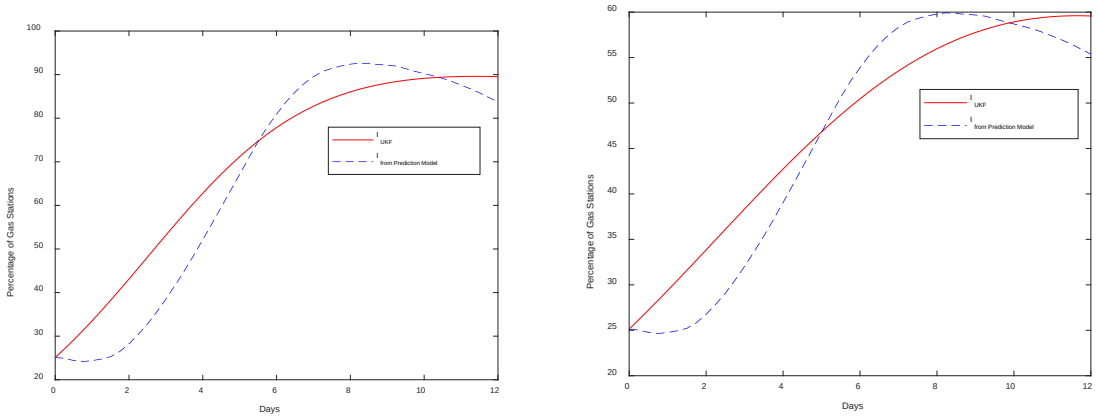

(a) (b)

Figure 2.4 Fuel shortage prediction model and the Time-invariant continuous SIR data computed using UKF parameter estimation for (a) category 3 hurricane and (b) category 1 hurricane.

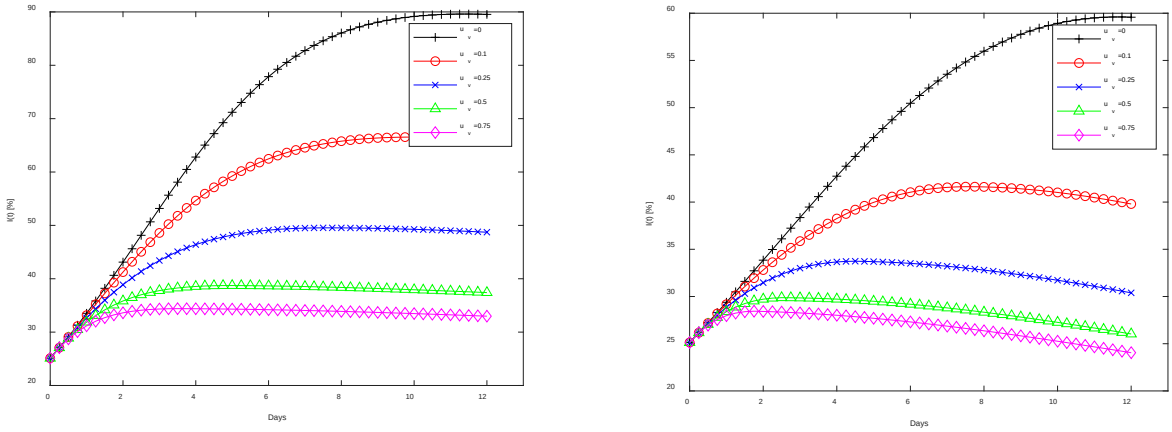

(a) (b)

Figure 2.5 Change in the percentage of empty fuel stations due to varying levels of intervention ($u_{v,max}$) for (a) Category 3 hurricane and (b) Category 1 hurricane

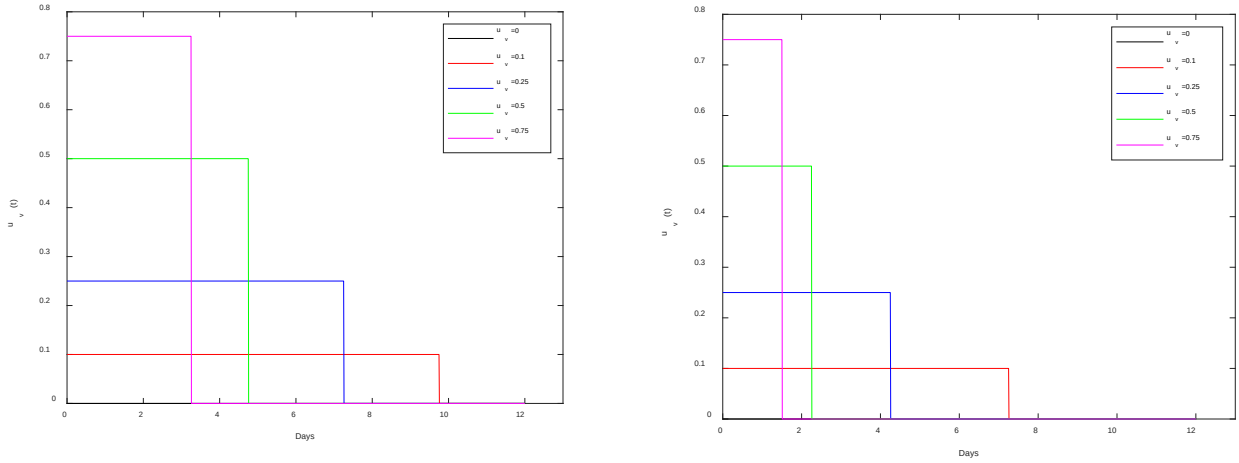

(a) (b)

Figure 2.6. Switching time of optimal refueling strategy for (a) category 3 and (b) category 1 hurricanes.

The initial data gathered during early stages of a hurricane evacuation can also be used as the measurement update of the UKF to evaluate the β parameter of the SIR dynamics model for fuel shortage. The γ parameter is related to recovery rate and can be estimated using the β estimate and an approximate recovery period based on historical data or by varying the R0. This analysis for all the affected regions combined with the optimal refueling methodology discussed above can help assess the levels of fuel supply required to mitigate the fuel shortage crisis in the affected regions, and thereby assist decision makers in allocating limited resources in a dynamically evolving emergency.

Figure 7 shows the predictive model for such case for Fort Myers-Naples area during Hurricane Irma. The R0 is valued to determine the recovery rate (γ) to produce the mechanistic data for the predictive model. For this analysis, it is assumed that Day 1 fuel shortage data for Fort Myers-Naples area is available and the parameter estimation applied to

it to determine the possible scenarios. The best fit R0 is the one that was determined as described is the methods section.

Figure 8 to 11 show the optimal refueling strategy for different R0s corresponding to figure 7 for Naples-Fort Myers. Figure 8 (a) shows the evolution of susceptible gas stations with different levels of intervention for R0=5. Similarly, figure 8(b) and (c) show the corresponding infected (or empty) gas stations and the switching time for various levels of intervention. Figures 9, 10 and 11 are similar plots for other values of R0. This approach can be applied during the early stages of an ongoing hurricane to establish upper and lower bounds for the possible levels of fuel shortage and to estimate the effect of various levels of intervention. The on-the-fly prediction will improve as more data becomes available.

CONCLUSIONS

In this paper, a predictive model formulation for the evolution of fuel shortages during hurricanes and an optimal control strategy to mitigate such shortages is presented. As fueling stations are depleted, their latent demand spreads to neighboring stations and throughout the community, similar to an epidemiological outbreak. This realization allows the application of well-established epidemiological research and models to be applied to fuel shortages and mitigation strategies. In addition, an epidemiological analogue for resource allocation based on vaccination models and optimal control theory is developed to address fuel shortages.

The data analysis of the evacuation traffic and crowd sourced fuel shortage data suggests that there is a direct correlation between the two. The analysis suggests the evacuation from Hurricane Irma and related activities depleted over 60 percent of the fuelling

stations in Tampa, Miami/Fort Lauderdale, and Naples, while Jacksonville saw depletion rates as high as 56 percent. Using epidemiological analogy, the fuel shortage epidemic is controlled when the basic reproduction number (R0) is less than 1. The predictive model suggests that there can be a fuel shortage in up to 90 percent of the refueling stations in Miami-Dade County, due to an evacuation from a Category 3 hurricane impacting Miami. The optimal control algorithm suggests the level and duration of intervention required to keep these fuel shortages from becoming an epidemic. While the application focused on hurricanes impacting Florida, the model is generally applicable to similar resource shortages due to evacuations in any location. The model can also be utilized to predict the level of fuel shortage and the effect of intervention, by using limited data available during the early stages of a hurricane evacuation. This approach is demonstrated using early data from Hurricane Irma for Naples-Fort Myers region.

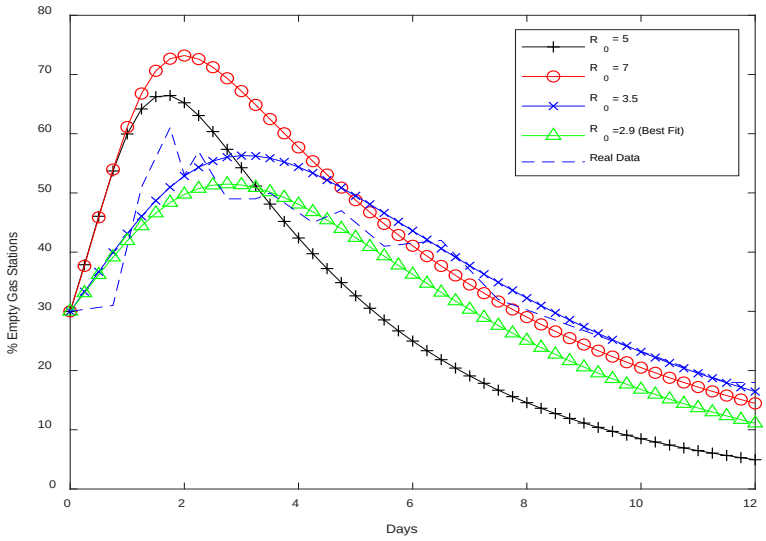

Figure 2.7. Predictive model for Fort Myers-Naples area from β parameter estimation and varied R0 of 7, 3.5 and 2.9 respectively.

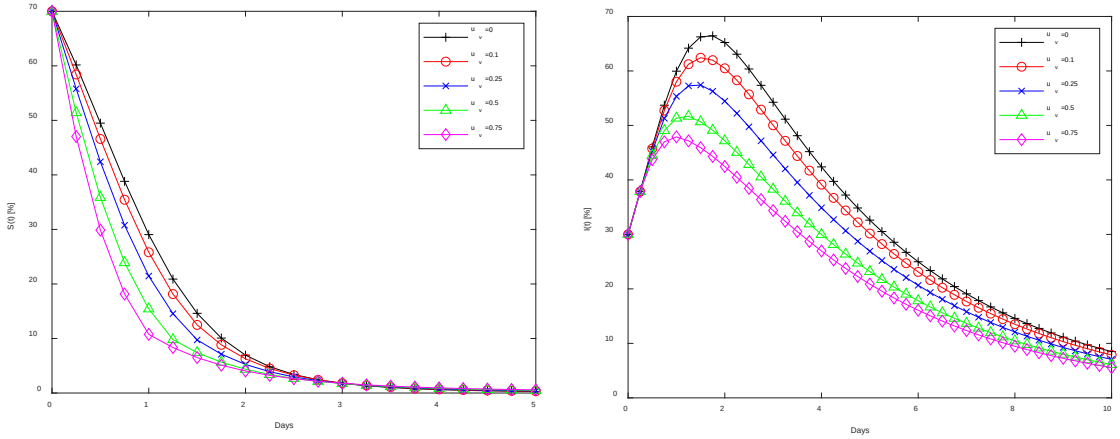

(a) (b)

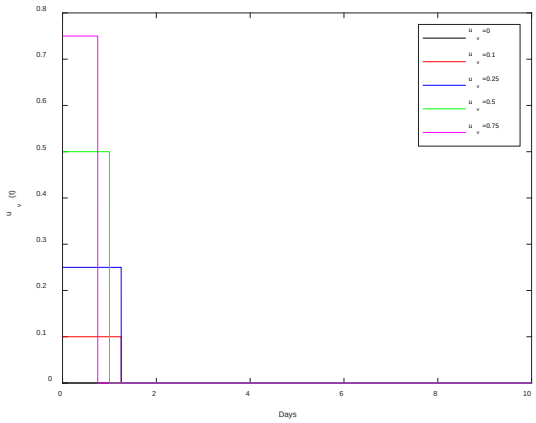

(c)

Figure 2.8. Evolution of (a) susceptible (operational), (b) infected (empty) gas stations, (c) The optimal application and switching time, t_s, for different refueling rates and the effect of refueling for Fort-Myers-Naples during Hurricane Irma for the predictive model with R_0=5.

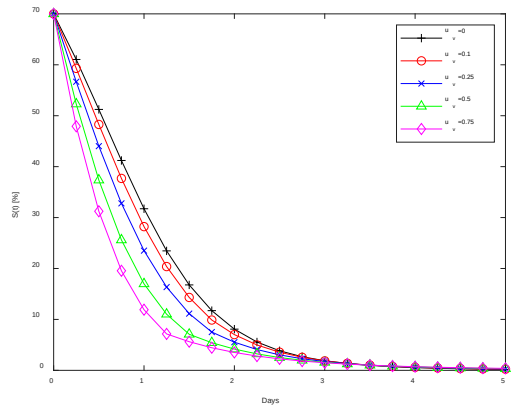

(a)

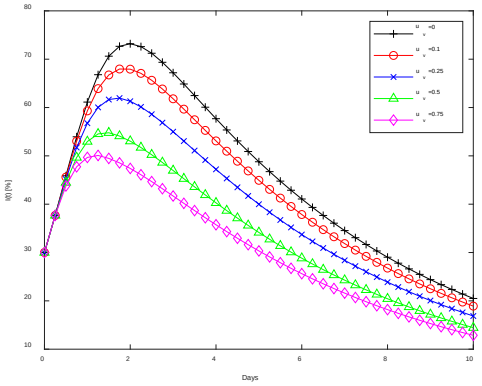

(b)

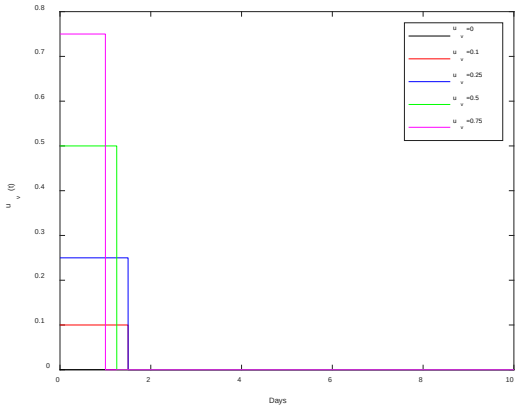

(c)

Figure 2.9. Evolution of (a) susceptible (operational), (b) infected (empty) gas stations, (c) The optimal application and switching time, t_s, for different refueling rates and the effect of refueling for Fort-Myers-Naples during Hurricane Irma for the predictive model with R_0=7.

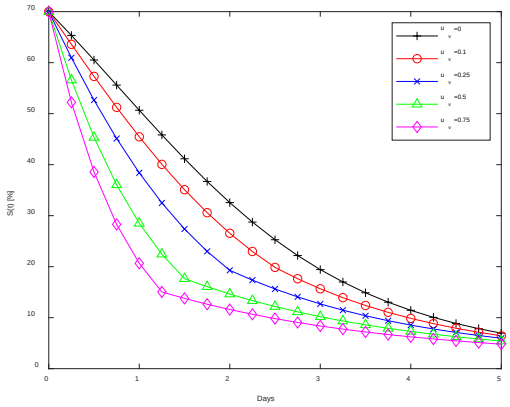

(b)

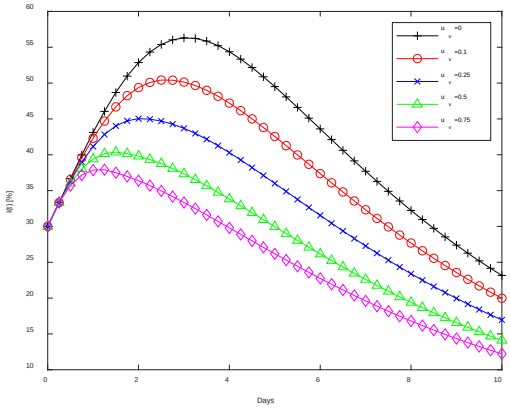

(a)

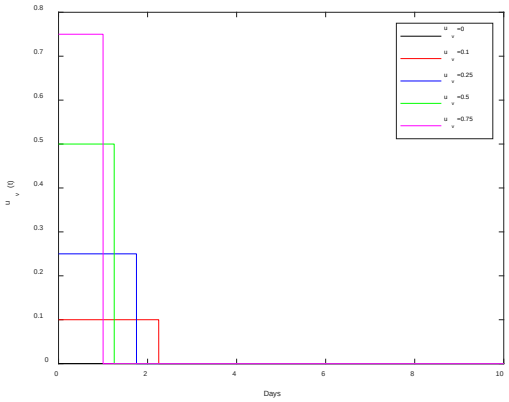

(c)

Figure 2.10. Evolution of (a) susceptible (operational), (b) infected (empty) gas stations, (c) The optimal application and switching time, t_s, for different refueling rates and the effect of refueling for Fort-Myers-Naples during Hurricane Irma for the predictive model with R_0=3.5.

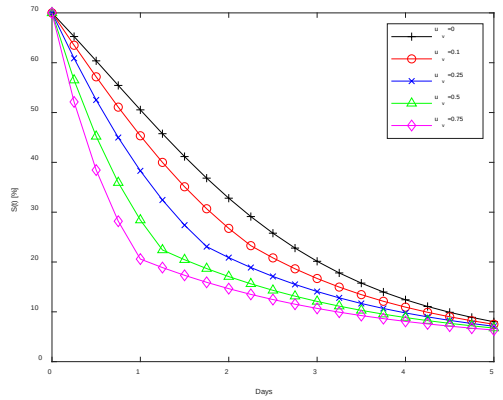

(a)

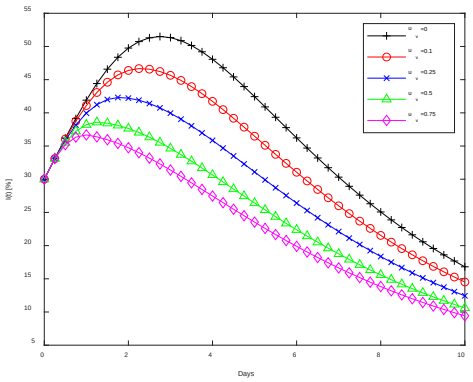

(b)

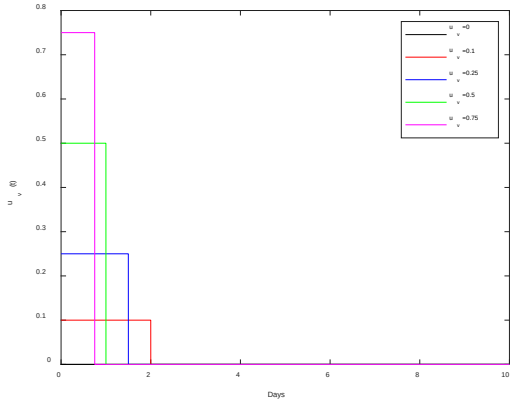

(c)

Figure 2.11. Evolution of susceptible (operational) gas stations and the effect of refueling for Fort-Myers-Naples during Hurricane Irma for the predictive model with R_0=2.9.

REFERENCES

1. Burn MJ, Palmer SE. Atlantic hurricane activity during the last millennium. Scientific reports. 2015 Aug 5;5:12838.
2. Holland G, Bruyère CL. Recent intense hurricane response to global climate change. Climate Dynamics. 2014 Feb 1;42(3-4):617-27.
3. Florida Department of Transportation (FDOT) Report. (2018). Hurricane Irma's Effect on Florida's Fuel Distribution System and Recommended Improvements.
4. News article : https://weather.com/safety/hurricane/news/2018-09-11-florence-evacuation-orders-states
5. News article: https://www.floridatoday.com/story/weather/hurricanes/2018/10/09/hurricane-michael-evacuations-residents-urged-leave/1574890002/
6. Cheng G, Wilmot CG, Baker EJ. A destination choice model for hurricane evacuation. In Proceedings of the 87th Annual Meeting Transportation Research Board, Washington, DC, USA 2008 Jan (pp. 13-17).
7. Khare A, He Q, Batta R. Predicting gasoline shortage during disasters using social media. OR Spectrum. 2019:1-34.
8. Gas Buddy website: https://gasbuddy.com/
9. Towers S, Gomez-Lievano A, Khan M, Mubayi A, Castillo-Chavez C. Contagion in mass killings and school shootings. PLoS one. 2015 Jul 2;10(7):e0117259.
10. Traag VA. Complex contagion of campaign donations. PloS one. 2016 Apr 14;11(4):e0153539.

11. Ferrara E, Yang Z. Measuring emotional contagion in social media. PloS one. 2015 Nov 6;10(11):e0142390.
12. Bearman PS, Moody J. Suicide and friendships among American adolescents. American journal of public health. 2004 Jan;94(1):89-95.
13. Liu W, Zhong S. Web malware spread modelling and optimal control strategies. Scientific reports. 2017 Feb 10;7:42308.
14. Tsvetkova M, Macy MW. The social contagion of generosity. PloS one. 2014 Feb 13;9(2):e87275.
15. Fu F, Christakis NA, Fowler JH. Dueling biological and social contagions. Scientific reports. 2017 Mar 2;7:43634.
16. Allen DJ, Brauer F, van den Driessche P, Wu J. Mathematical epidemiology. Berlin: Springer; 2008.
17. Yang K, Wang E, Zhou Y, Zhou K. Optimal vaccination policy and cost analysis for epidemic control in resource-limited settings. Kybernetes. 2015 Mar 2;44(3):475-86.
18. Hansen E, Day T. Optimal control of epidemics with limited resources. Journal of mathematical biology. 2011 Mar 1;62(3):423-51.
19. https://www.wsj.com/articles/gasbuddy-app-scores-big-during-florida-fuel-shortage-1504954805
20. Levin N, Lechner AM, Brown G. An evaluation of crowdsourced information for assessing the visitation and perceived importance of protected areas. Applied geography. 2017 Feb 1;79:115-26.

21. National Hurricane Center. (2017, November). Irma Graphics Archive: 5-Day Forecast Track and Watch/Warning Graphic.
22. Florida Department of Transportation SunGuide Program. https://www.fdot.gov/traffic/its/projects-arch/sunguide.shtm
23. United States Census Bureau, https://factfinder.census.gov/faces/tableservices/jsf/pages/productview.xhtml?pid=ECN_2012_US_00A1&prodType=table
24. Kalman RE. A new approach to linear filtering and prediction problems. Journal of basic Engineering. 1960 Mar 1;82(1):35-45.
25. Kalman RE, Bucy RS. New results in linear filtering and prediction theory. Journal of basic engineering. 1961 Mar 1;83(1):95-108.
26. Grewal MS, Andrews AP. Applications of Kalman filtering in aerospace 1960 to the present [historical perspectives]. IEEE Control Systems Magazine. 2010 May 18;30(3):69-78.
27. Chang CB, Athans M, Whiting R. On the state and parameter estimation for maneuvering reentry vehicles. IEEE Transactions on Automatic Control. 1977 Feb;22(1):99-105.
28. Langelaan JW. State estimation for autonomous flight in cluttered environments. Journal of guidance, control, and dynamics. 2007 Sep;30(5):1414-26.
29. Yang W, Karspeck A, Shaman J. Comparison of filtering methods for the modeling and retrospective forecasting of influenza epidemics. PLoS computational biology. 2014 Apr 24;10(4):e1003583.

30. Costa PJ, Dunyak JP, Mohtashemi M. Models, prediction, and estimation of outbreaks of infectious disease. InProceedings. IEEE SoutheastCon, 2005. 2005 Apr 8 (pp. 174-178). IEEE.
31. Sabet MT, Sarhadi P, Zarini M. Extended and Unscented Kalman filters for parameter estimation of an autonomous underwater vehicle. Ocean Engineering. 2014 Nov 15;91:329-39.
32. Musoff H, Zarchan P. Fundamentals of Kalman filtering: a practical approach. American Institute of Aeronautics and Astronautics; 2009 Aug 29.
33. Evensen G. The ensemble Kalman filter: Theoretical formulation and practical implementation. Ocean dynamics. 2003 Nov 1;53(4):343-67.
34. Wan, E.A. and Van Der Merwe, R., "The Unscented Kalman Filter for Nonlinear Estimation", Proceedings of the IEEE 2000 Adaptive Systems for Signal Processing, Communications, and Control Symposium, 2000.
35. Julier S, Uhlmann J, Durrant-Whyte HF. A new method for the nonlinear transformation of means and covariances in filters and estimators. IEEE Transactions on automatic control. 2000 Mar;45(3):477-82.
36. Lewis FL, Vrabie D, Syrmos VL. Optimal control. John Wiley & Sons; 2012 Mar 20.
37. Lee S, Cochran JE. Orbital maneuvers via feedback linearization and bang-bang control. Journal of guidance, control, and dynamics. 1997 Jan;20(1):104-10.

38. Singh G, Kabamba PT, McClamroch NH. Bang-bang control of flexible spacecraft slewing maneuvers: guaranteed terminal pointing accuracy. Journal of Guidance, Control, and Dynamics. 1990 Mar;13(2):376-9.
39. Pontryagin LS. Mathematical theory of optimal processes. Routledge; 2018 May 3.
40. Baker, E. 2010. Statewide Regional Evacuation Study Program: Volume 2-11 South Florida Region Regional Behavioral Analysis (United States, Florida Division of Emergency Management, South Florida Regional Planning Council). Tallahassee, FL. Retrieved July 19, 2019, from http://www.sfrpc.com/SRESP Web/Vol2-11.pdf
41. Laura Bliss. (2017). Why Florida Ran Out of Gas. Retrieved:https://www.citylab.com/transportation/2017/09/why-florida-ran-out-of-gas/539541/.
42. Yin, W., Murray-Tuite, P., Ukkusuri, S.V. and Gladwin, H., 2014. An agent-based modeling system for travel demand simulation for hurricane evacuation. Transportation research part C: emerging technologies, 42, pp.44-59.
43. Centola, D. (2011). An experimental study of homophily in the adoption of health behavior. Science, 334(6060), 1269-1272.
44. Gao, L., Wang, W., Pan, L., Tang, M., & Zhang, H. F. (2016). Effective information spreading based on local information in correlated networks. Scientific reports, 6, 38220.

45. Christakis, N. A., & Fowler, J. H. (2007). The spread of obesity in a large social network over 32 years. New England journal of medicine, 357(4), 370-379.
46. Dong, S., Fan, F. H., & Huang, Y. C. (2018). Studies on the population dynamics of a rumor-spreading model in online social networks. Physica A: Statistical Mechanics and its Applications, 492, 10-20.
47. Watts, D. J., & Dodds, P. S. (2007). Influential, networks, and public opinion formation. Journal of consumer research, 34(4), 441-458.
48. Fu, F., Christakis, N.A. and Fowler, J.H., 2017. Dueling biological and social contagions. Scientific reports, 7, p.43634.
49. Towers, S., Afzal, S., Bernal, G., Bliss, N., Brown, S., Espinoza, B., Jackson, J., Judson-Garcia, J., Khan, M., Lin, M. and Mamada, R., 2015. Mass media and the contagion of fear: the case of Ebola in America. Plos One, 10(6), p.e0129179.
50. Sprague, D.A. and House, T., 2017. Evidence for complex contagion models of social contagion from observational data. Plos One, 12(7), p.e0180802.
51. FEMA. (2018). 2017 hurricane season FEMA after-action report (United States, FEMA). Washington D.C. Retrieved July, 2018, Retrieved from: https://www.fema.gov/medialibrarydata/1531743865541d16794d43d3082544435e1471da07880/2017FEMAHurricaneAAR.pdf

52. Murray-Tuite, P., Yin, W., Ukkusuri, S. V., & Gladwin, H. (2012). Changes in evacuation decisions between Hurricanes Ivan and Katrina. Transportation research record, 2312(1), 98-107.
53. Lindell, M. K., & Prater, C. S. (2007). Critical behavioral assumptions in evacuation time estimate analysis for private vehicles: Examples from hurricane research and planning. Journal of Urban Planning and Development, 133(1), 18-29.
54. Downs, P., Prusaitis, S., Germain, J., and J. Baker. 2010. Statewide Regional Evacuation Study Program: Volume 3-11 South Florida Region Regional Behavioral Survey Report (United States, Florida Division of Emergency Management, South Florida Regional Planning Council). Tallahassee, FL. Retrieved July 19, 2019, Retrieved from: http://www.sfrpc.com/SRESPWeb/Vol3-11.pdf
55. Dow, K., & Cutter, S. L. (2002). Emerging hurricane evacuation issues: hurricane Floyd and South Carolina. Natural hazards review, 3(1), 12-18.
56. Wu, H. C., Lindell, M. K., & Prater, C. S. (2012). Logistics of hurricane evacuation in Hurricanes Katrina and Rita. Transportation research part F: traffic psychology and behaviour, 15(4), 445-461.
57. Wolshon, B. (2008). Empirical characterization of mass evacuation traffic flow. Transportation research record, 2041(1), 38-48.

58. Li, J., Ozbay, K., Bartin, B., Iyer, S., & Carnegie, J. A. (2013). Empirical evacuation response curve during Hurricane Irene in Cape May County, New Jersey. Transportation research record, 2376(1), 1-10.

59. Li, J., & Ozbay, K. (2015). Hurricane Irene evacuation traffic patterns in New Jersey. Natural Hazards Review, 16(2), 05014006.

60. Li, J., Ozbay, K., & Bartin, B. (2015). Effects of Hurricanes Irene and Sandy in New Jersey: traffic patterns and highway disruptions during evacuations. Natural Hazards, 78(3), 2081-2107.

61. Lewis, F. L., Vrabie, D., & Syrmos, V. L. (2012). Optimal control. John Wiley & Sons.

62. Islam, S., Namilae, S., Prazenica, R., & Liu, D. (2020). Fuel shortages during hurricanes: Epidemiological modeling and optimal control. Plos one, 15(4), e0229957.

63. U.S. Census Bureau QuickFacts: Broward County, Florida. (2018). Retrieved July 19, 2019, Retrieved from: https://www.census.gov/quickfacts/browardcountyflorida

64. National Hurricane Center. (2017, November). Irma Graphics Achive: 5-Day Forecast Track and Watch/Warning Graphic. Retrieved July, 2018, from: https://www.nhc.noaa.gov/archive/2017/IRMA_graphics.php?product=5day_cone_with_line